Published in final edited form as:

Nat Med. 2020 April ; 26(4): 608–617. doi:10.1038/s41591-020-0764-0.

Interleukin-22-mediated host glycosylation prevents *Clostridioides difficile* infection by modulating the metabolic activity of the gut microbiota

Hiroko Nagao-Kitamoto[1], **Jhansi L. Leslie**[2,3,*], **Sho Kitamoto**[1], **Chunsheng Jin**[4], **Kristina A. Thomsson**[4], **Merritt G. Gillilland III**[1], **Peter Kuffa**[1], **Yoshiyuki Goto**[5,6,7], **Robert R. Jenq**[8], **Chiharu Ishii**[9], **Akiyoshi Hirayama**[9], **Anna M. Seekatz**[2,#], **Eric C. Martens**[3], **Kathryn A. Eaton**[3], **John Y. Kao**[1], **Shinji Fukuda**[9,10,11,12], **Peter D. R. Higgins**[1], **Niclas G. Karlsson**[4], **Vincent B. Young**[2,3], **Nobuhiko Kamada**[1]

[1]Division of Gastroenterology, University of Michigan Medical School, Ann Arbor, Michigan, USA

[2]Division of Infectious Disease, Department of Internal Medicine, University of Michigan Medical School, Ann Arbor, Michigan, USA

[3]Department of Microbiology and Immunology, University of Michigan Medical School, Ann Arbor, Michigan, USA

[4]Institute of Biomedicine, Department of Medical Biochemistry, University of Gothenburg, 405 30 Gothenburg, Sweden

[5]Division of Molecular Immunology, Medical Mycology Research Center, Chiba University, Chiba 260-8673, Japan

[6]Division of Mucosal Symbiosis, International Research and Development Center for Mucosal Vaccines, Institute of Medical Science, The University of Tokyo, Tokyo 108-8639, Japan

[7]AMED-PRIME, Japan Agency for Medical Research and Development, Tokyo 100-0004, Japan

[8]Department of Genomic Medicine, Division of Cancer Medicine, University of Texas MD Anderson Cancer Center, Houston, Texas, USA

[9]Institute for Advanced Biosciences, Keio University, Tsuruoka 997-0052, Japan

[10]Intestinal Microbiota Project, Kanagawa Institute of Industrial Science and Technology, Ebina 210-0821, Japan

Address correspondence to: Nobuhiko Kamada, Division of Gastroenterology, Department of Internal Medicine, University of Michigan, 1150 W. Medical Center Drive, Ann Arbor, MI 48109. nkamada@umich.edu.

*current address: The University of Virginia

#current address: Clemson University

Authorship Contributions:

H.N.-K. and N.K. conceived and designed experiments. H.N.-K. conducted most of the experiments with help from J.L.L., S.K., P.K., and A.M.S.. M.G.G. performed microbiome analysis. C.I., A.H., and S.F. performed metabolome analysis. K.A.E. helped with germ-free animal experiments. P.D.R.H. provided human stool samples. C.J., K.A.T and N.G.K. conducted glycan analysis. Y.G., R.R.J., V.B.Y., E.C.M. and J.Y.K. helped with critical advice and discussion. H.N.-K. and N.K. analyzed the data. H.N.-K. and N.K. wrote the manuscript with contributions from all authors.

Disclosures: The authors declare no competing interests.

[11]Transborder Medical Research Center, University of Tsukuba, Tsukuba 305-8575, Japan

[12]PRESTO, Japan Science and Technology Agency, Kawaguchi 332-0012, Japan

Abstract

The involvement of host immunity in the gut microbiota-mediated colonization resistance to *Clostridioides difficile* infection (CDI) is incompletely understood. Here, we show that interleukin (IL)-22, induced by colonization of the gut microbiota, is crucial for the prevention of CDI in human microbiota-associated (HMA) mice. IL-22 signaling in HMA mice regulated host glycosylation, which enabled the growth of succinate-consuming bacteria *Phascolarctobacterium* spp. within the gut microbiome. *Phascolarctobacterium* reduced the availability of luminal succinate, a crucial metabolite for the growth of *C. difficile*, and therefore prevented the growth of *C. difficile*. IL-22-mediated host *N*-glycosylation is likely impaired in patients with ulcerative colitis (UC), and renders UC-HMA mice more susceptible to CDI. Transplantation of healthy human-derived microbiotas or *Phascolarctobacterium* reduced luminal succinate levels and restored colonization resistance in UC-HMA mice. IL-22-mediated host glycosylation thus fosters the growth of commensal bacteria that compete with *C. difficile* for the nutritional niche.

Introduction

Clostridioidies difficile infection (CDI) causes a severe, potentially life-threatening intestinal inflammation in hospitalized patients [1]. The gut microbiota plays a central role in the prevention of CDI, as antibiotic treatment promotes the growth of *C. difficile*, resulting in the development of CDI [1]. However, the precise mechanism by which constituents of healthy microbiotas outcompete *C. difficile* is not fully understood. Healthy gut microbiotas directly prevent *C. difficile* from blooming in the gut via increasing the abundance of metabolites that interfere with the growth of *C. difficile* or decreasing the availability of germination/growth-promoting luminal metabolites required by *C. difficile* [2, 3]. Besides their metabolic functions, the gut microbiotas are also known to activate host antimicrobial immunity, which, in turn, indirectly prevents the colonization and/or growth of many enteric pathogens [4]. Despite this fact, the role of host immunity-mediated colonization resistance in CDI, conferred by the gut microbiota, remains underappreciated.

Accumulating evidence has suggested that IL-22 plays a pivotal role in mucosal defense mechanisms in the gastrointestinal tract through promotion of epithelial barrier integrity, secretion of antimicrobial peptides, and induction of iron scavengers [5, 6, 7]. Moreover, IL-22 modulates host epithelial glycosylation, which, in turn, prevents the growth of enteric pathogens, such as *Citrobacter rodentium* and *Salmonella* [8, 9, 10]. In the gut, IL-22 production is regulated by the resident microbiota [11, 12], indicating that IL-22 induction is a mechanism utilized by the gut microbiota to mediate colonization resistance against enteric pathogens. Previous studies have demonstrated that IL-22 is not required for the prevention of *C. difficile* growth in the intestine [13, 14, 15]. However, in these studies, the intestinal microbiota was depleted by treatment with antibiotics prior to CDI, and therefore, microbiota-dependent induction of IL-22 may not have been detected in their models. Thus, the involvement of a microbiota-induced IL-22 pathway and the contribution of its defects to

the increased risk of CDI remain largely unknown. Herein, we report that mucosal IL-22 signaling, activated by the colonization of the gut microbiota, modulated glycosylation of host *N*-linked glycans. Host-derive glycans, in turn, promote the growth of succinate-consuming bacteria *Phascolarctobacterium* spp.. *Phascolarctobacterium* spp. consumed succinate, a metabolite that fuels *C. difficile*, thereby preventing the growth of *C. difficile* in the intestine. Of note, The IL-22-mediated regulation of host *N*-glycans is likely impaired in patients with ulcerative colitis (UC), and thereby leading to gut dysbiosis with altered microbial metabolic activities, including succinate metabolism. Hence, gnotobiotic mice that harbor the gut microbiota from UC patients were susceptible to CDI. Thus, IL-22-mediated host glycosylation fosters the growth of commensal bacteria that compete with *C. difficile* for the nutritional niche, and the defects in this pathway might increase the risk for CDI.

Results

Human microbiotas protect germ-free mice from CDI

We examined the protective role of human-derived microbiotas against CDI. GF mice were colonized with the gut microbiotas isolated from two healthy controls (HC). HC human microbiota-associated (HC-HMA) mice [16] were infected with *C. difficil*e strain VPI 10463. As a control, GF mice without microbiota reconstitution were also infected with *C. difficile*. *C. difficile* was able to colonize control GF mice 1 day after infection and the following day all mice succumbed to CDI (Extended Data Fig. 1a). Consistent with a previous report [17], HC-HMA mice were completely protected against CDI and *C. difficile* was unable to colonize these mice (Extended Data Fig. 1a). In order to confirm the importance of the gut microbiota, we next treated HC-HMA mice with a broad-spectrum antibiotic cocktail [17]. As expected, marked *C. difficile* colonization ($>10^7$–10^8 CFU/g feces) was observed in antibiotic-treated HC-HMA mice starting on day 1 post-CDI and the majority of mice succumbed to CDI (Extended Data Fig. 1b). Consistent with fecal pathogen burden data, antibiotic-treated HC-HMA mice developed inflammatory pathology in the colon, while no overt inflammation was observed in control HC-HMA mice (Extended Data Fig. 1c). These data suggest that human-derived microbiotas confer colonization resistance against *C. difficile* in mice.

Microbiota-induced IL-22 prevents CDI

Rag1$^{-/-}$ mice, which lack both T and B cells were used to address the role of host immunity in the human microbiota-conferred colonization resistance against *C. difficile*. GF *Rag1*$^{-/-}$ mice were colonized by HC microbiotas to generate HC-HMA-*Rag1*$^{-/-}$ mice. HC-HMA-*Rag1*$^{-/-}$ mice and control GF *Rag1*$^{-/-}$ mice were infected with *C. difficile*. All GF *Rag1*$^{-/-}$ mice succumbed to CDI within 2 days of infection. In contrast, *C. difficile* was unable to grow in HC-HMA-*Rag1*$^{-/-}$ mice, as was seen in HC-HMA-WT mice (Fig. 1a). This result indicated that host T and B cell immunity is not required for the human microbiota to confer resistance against *C. difficile*. Rather, the host's innate antimicrobial response, elicited by the microbiota, plays a role in the prevention of CDI. In this regard, we found that colonization of GF *Rag1*$^{-/-}$ mice with human microbiotas induced mucosal IL-22 expression (Fig. 1b). This evidence hinted at the involvement of IL-22 in a mechanism underlying microbiota-mediated protection against CDI. To test this hypothesis, we

examined the impact of IL-22 signaling blockade in HC-HMA-*Rag1*$^{-/-}$ mice on CDI susceptibility (Fig. 1c). IL-22 signaling was efficiently inhibited by an αIL-22 antibody *in vivo*. The antibody treatment also suppressed the expression of *Reg3b* and *Reg3g*, two antimicrobial proteins that are strongly induced in response to IL-22 [18] (Extended Data Fig. 2). In this setting, colonization resistance of HC-HMA-*Rag1*$^{-/-}$ mice was abolished and *C. difficile* was able to colonize the IL-22–neutralized HC-HMA-*Rag1*$^{-/-}$ mice (Fig. 1c). In accordance with its colonization potential, *C. difficile* induced massive inflammation in HC-HMA-*Rag1*$^{-/-}$ mice when IL-22 signaling was blocked (Fig. 1d). Thus, the microbial induction of IL-22 is critical for the prevention of *C. difficile* blooms in HMA mice.

IL-22 shapes the gut microbial community and its metabolic function

We next sought to study the mechanism by which IL-22 prevents CDI and examine the effect of IL-22 on the composition of the gut microbial community. We analyzed the gut microbiome of HC-HMA-*Rag1*$^{-/-}$ mice treated with the αIL-22 antibody. IL-22 neutralization did not change the diversity and richness of the microbial communities (Extended Data Fig. 3a), but did change the composition of the gut microbiota (Extended Data Fig. 3b). In particular, it resulted in a decrease in the abundance of *Acidaminococcaceae* following IL-22 neutralization (Extended Data Fig. 3c). LEfSe analysis further identified bacterial genera that became over- and under-represented following IL-22 neutralization (Fig. 2a). Among them, we focused on genus *Phascolarctobacterium* (family *Acidaminococcaceae*), which was significantly decreased as a result of IL-22 blockade (Fig. 2a). *Phascolarctobacterium* spp. are the major consumers of succinate generated by other bacterial species, such as *Bacteroides* spp. [19, 20]. Thus, the decreased abundance of *Phascolarctobacterium* may lead to abnormal succinate metabolism in the gut. Consistent with this hypothesis, the luminal levels of succinate were significantly elevated in IL-22-neutralized HC-HMA-*Rag1*$^{-/-}$ mice (Fig. 2b, Extended Data Fig. 4, and Supplementary Table 1). Importantly, luminal succinate is known to aid the growth of *C. difficile* in the intestine [21]. Hence, an imbalance in succinate metabolism due to gut dysbiosis, induced by a blockade of IL-22 signaling, may affect the host's susceptibility to CDI. To explore this notion, we utilized a mutant strain of *C. difficile* that lacks the succinate utilization gene operon CD2344 [21]. The CD2344 mutant of *C. difficile* (*Cd-CD2344*$^{-}$), unlike its isogenic WT strain JIR8094, is unable to grow on succinate (Extended Data Fig. 5) [21]. IL-22-neutralized HC-HMA-*Rag1*$^{-/-}$ mice, which are susceptible to CDI, were infected with either WT JIR8094 or *Cd-CD2344*$^{-}$ (Fig. 2c). As seen in Fig. 1, WT *C. difficile* was able to colonize IL-22-neutralized HC-HMA-*Rag1*$^{-/-}$ mice (Fig. 2c). In contrast, early colonization by *Cd-CD2344*$^{-}$ was markedly impaired (Fig. 2c). To address the extent to which succinate plays a key role in the increased susceptibility to CDI, we administrated succinate to HC-HMA mice. We observed that the administration of succinate promoted the growth of *C. difficile* in HC-HMA mice (Fig. 2d), indicating that succinate is a key metabolite whose abundance controls the colonization of *C. difficile* in the gut. Interestingly, *Cd-CD2344*$^{-}$ was able to colonize in GF mice (Extended Data Fig. 6), suggesting that *C. difficile* can utilize alternate nutritional sources for its growth in the absence of commensal microbiota. Next, we asked if colonization by the succinate-consuming bacteria *Phascolarctobacterium* spp. can prevent CDI. Specific pathogen-free (SPF) C57BL/6 mice were pre-treated with cefoperazone to breach the gut colonization

resistance [3]. As previously reported, the cefoperazone-treated mice succumbed to CDI (Fig. 2e). Colonization by two strains of *Phascolarctobacterium* – *P. faecium* JCM 30894 and *P. succinatutens* JCM 16074 – significantly improved mortality of *C. difficile*–infected mice (Fig. 2e). These results suggest that IL-22, induced by the microbiota, modulates the abundance of specific commensal bacteria, such as *Phascolarctobacterium*, and can lead to the accumulation of luminal metabolites, including succinate, which may foster the growth of *C. difficile*.

Host mucus glycosylation regulates gut microbiota

Given the decreased abundance of succinate-consuming bacteria *Phascolarctobacterium* in the gut significantly decreased when IL-22 signaling was blocked, it is conceivable that IL-22 signaling promotes the growth of *Phascolarctobacterium* in the gut. To test this hypothesis, GF mice were colonized with two strains of *Phascolarctobacterium*, *P. faecium* JCM 30894, and *P. succinatutens* JCM 16074, followed by treatment with an IL-22-Fc fusion protein. The amount of host genomic DNA in feces remained unchanged as a result of rIL-22 treatment (Fig. 3a). The gut colonization of both strains (gene copies normalized to host genomic DNA) was significantly enhanced by IL-22-Fc, suggesting that IL-22 directly regulates the growth of *Phascolarctobacterium* (Fig. 3a). The growth of *Phascolarctobacterium* is primarily limited by the availability of succinate, while carbohydrates and/or SCFAs do not appear to be of major importance [19]. However, succinate is not available in GF mice since succinate-producing commensal bacteria are absent [21]. This indicates that *Phascolarctobacterium* can utilize other nutritional sources for its growth in gnotobiotic mice treated with IL-22-Fc. We found that *P. faecium* JCM 30894 and *P. succinatutens* JCM 16074 harbors enzymes that belong to glycoside hydrolase (GH) families, GH73 (GenBank/EMBL/DDBJ accession# AB490811). Given that GH73 is a member of the host glycan-related enzyme families (*N*-acetylglucosamine (GlcNAc)), it is plausible that *Phascolarctobacterium* has become adapted to consume host-derived glycans in the gut. To examine this, we isolated mucus from SPF mice treated with the αIL-22 antibody or the isotype control antibody. Isolated mucus was added to the *Phascolarctobacterium* growth medium *in vitro*. Supplementation with mucus isolated from control mice promoted the growth of *P. faecium* and *P. succinatutens* (Fig. 3b). In contrast, the growth of *P. faecium* and *P. succinatutens* was significantly weakened when mucus isolated from IL-22–neutralized mice was used (Fig. 3b). Consistent with this result, *P. faecium* and *P. succinatutens* expressed GH73 when cultured in mucus (Fig. 3c). Moreover, supplementation with GlcNAc enhanced the growth of *Phascolarctobacterium* (Fig. 3d). These results suggest that IL-22–induced host mucus glycosylation likely promotes the growth of *Phascolarctobacterium*. We also assessed the expression of host glycosyltransferases in HC-HMA mice, and whether or not these enzymes are regulated *via* IL-22 signaling. As shown in Fig. 3e, host glycosyltransferases that are related to *N*-glycosylation, such as *Mgat4a*, were induced in GF mice upon colonization with a human microbiota. The microbiota-induced IL-22 was responsible for the induction of some of these enzymes, as their expression levels were significantly reduced when IL-22 signaling was blocked (Fig. 3e). We next analyzed the host glycosylation status of HMA-*Rag1*$^{-/-}$ mice with or without IL-22 signal blockade. We found that *N*-glycosylation of the host proteins was impaired in IL-22-neutralized mice both in the insoluble fractions (mainly mucus

proteins, such as Muc2) and in the soluble fractions (intestinal cells, such as epithelial cells). Notably, high-mannose glycans were reduced in the soluble fraction and hybrid glycans tended to be decreased in the insoluble fraction in IL-22–neutralized mice (Fig. 3f, g, and Supplementary Table 2). In contrast, O-glycisylation was unchanged in IL-22-neutralized mice (Supplementary Table 3). These findings suggest that IL-22–mediated host *N*-glycosylation may foster the growth of some commensal microbiota, such as *Phascolarctobacterium*.

Impaired N-glycosylation–related gene expression in UC patients

We next examined the link between IL-22–mediated host glycosylation and increased host susceptibility to CDI resulting from underlying disease. To this end, we focused on patients with ulcerative colitis (UC), who are at higher risk for CDI compared to normal individuals [22, 23, 24]. Using a publically available database (GSE75214) [25], we found that the expression of host glycosyltransferases, such as *MGTA4A* and *MGAT4B*, was significantly impaired in UC patients compared to normal controls (Fig. 4a). The expression of *IL22RA2* (also known as IL-22 binding protein (IL-22BP), a soluble IL-22 receptor that blocks IL-22 signaling, was markedly up-regulated in patients with UC, while IL-22 expression was not affected (Fig. 4a and Extended Data Fig. 7a). Notably, *IL22RA2* expression was inversely correlated with the expression of these glycosyltransferases, indicating that impaired IL-22 signaling, resulting from the overexpression of IL-22BP, led to decreased host glycosylation in UC (Fig. 4b). An analysis of two other deposited cohorts (GSE16879 [26] and GSE73661 [27]) revealed similar expression patterns, and inverse correlation between *IL22RA2* and host glycosylation enzymes (Extended Data Fig. 7b-e). Consistent with these results, HMA mice-colonized with the microbiotas derived from UC patients (UC-HMA mice) were unable to resist *C. difficile* colonization (Fig. 4c, 4d). Consistent with the *in vivo* data, inoculated *C. difficile* failed to proliferate *ex vivo* using luminal contents isolated from HC-HMA mice (Fig. 5a). On the other hand, *C. difficile* grew from luminal contents isolated from UC-HMA mice (Fig. 5a). As expected, the growth of *C. difficile* was dependent on succinate, as the *Cd-CD2344*$^{-}$ mutant exhibited impaired growth in UC luminal contents *in vitro* and *in vivo* (Fig. 5b, c).

Restoration of microbial metabolism reduces the risk for CDI

Finally, we tested whether fecal microbiota transplantation (FMT) could restore normal microbial metabolic activity and colonization resistance in UC-HMA mice. Healthy human-derived microbiotas were inoculated into UC-HMA mice, which were then infected with *C. difficile* (Fig. 6a). As a result, FMT almost completely prevented the growth of *C. difficile* in the gut (Fig. 6b). We found that a single FMT was equally effective at preventing CDI as multiple FMTs (Fig. 6b). Gut dysbiosis seen in UC-HMA mice improved significantly as a result of FMT (Fig. 6c–6e), which restored the abundance of *Phascolarctobacterium* (Fig. 6f and Extended Data Fig. 8). Consistent with this, the levels of luminal succinate were significantly reduced following FMT (Fig. 6g, Extended Data Fig. 9, and Supplementary Table 4). To validate the importance of *Phascolarctobacterium* in the prevention of CDI, we inoculated UC-HMA mice with succinate consumers, *P. faecium* and *P. succinatutens,* instead of a full FMT (Fig. 6h). As expected, colonization of *P. faecium* and *P. succinatutens* significantly reduced the concentration of luminal succinate (Fig. 6i). According to the

reduction of luminal succinate availability, Inoculation of *Phascolarctobacterium* significantly inhibited the colonization of *C. difficile*, particularly in early stages of infection (Fig. 6j).

Discussion

By utilizing the HMA mouse model, we demonstrated that IL-22, induced by colonization of the gut microbiota, shapes the composition of the gut resident microbiota. IL-22 signaling promotes the expression of host glycosyltransferases, such as *Mgat4a* and *Mgat4b*, which encode enzymes that catalyze the transfer of *N*-acetylglucosamine (GlcNAc) to the core mannose residues[28, 29]. The overall abundance of GlcNAc seemed unchanged, although *N*-glycosylation in both soluble and insoluble fraction of mucus was compromised by the impairment of IL-22 signaling. This suggests that the transfer of GlcNAc to *N*-linked glycans may be impaired only in subsets of host-derived proteins. Host glycosylation plays an important role in maintaining specific populations of gut commensal bacteria, such as *Phascolarctobacterium* spp., which utilize host-derived GlcNAc for their growth[19, 30]. The dysbiotic microbiota, as a result of the impaired IL-22 signaling, has a compromised metabolic function, thereby increasing the opportunistic growth of potential pathogens, such as *C. difficile*.

It has been reported that the abundance of *Phascolarctobacterium* is markedly reduced in CDI patients compared to healthy control subjects [31]. Likewise, the abundance of *Phascolarctobacterium* was restored in CDI patients following FMT, resulting in the amelioration of their clinical symptoms [32]. Thus, the abundance of *Phascolarctobacterium* is likely involved in host protection against CDI. However, the mechanisms by which *Phascolarctobacterium* spp. are regulated within the gut microbiota remain poorly understood. In this study, we found that *Phascolarctobacterium* spp. harbor glycoside hydrolases associated with host glycan degradation, suggesting that *Phascolarctobacterium* spp. have the ability to forage host glycans in addition to consuming succinate. Therefore, IL-22-mediated host *N*-glycosylation likely promotes the growth of this bacterial genus in the gut. We speculate that the increased abundance of *Phascolarctobacterium* spp. leads to a more efficient consumption of succinate in the gut lumen, which limits the opportunistic growth of *C. difficile* whose proliferation is aided by succinate [21]. Interestingly, the administration of *Phascolarctobacterium* spp. sufficiently protects antibiotic-treated mice from CDI. Further, *Phascolarctobacterium* improves the mortality of infected animals, even if they are inoculated after the colonization by *C. difficile* (Extended Data Fig. 10). These data suggest that *Phascolarctobacterium* might be useful for treating patients who are already infected with *C. difficile*. However, it is noteworthy that single-dose, pre-treatment with *Phascolarctobacterium* was not sufficient to prevent *C. difficile* colonization and subsequent lethal colitis (Extended Data Fig. 10), suggesting that *Phascolarctobacterium* must retain an optimal number in the intestine to maximize their protective effect against CDI.

Phascolarctobacterium spp. are not the only bacterial species regulated by IL-22–mediated gut conditioning. LEfSe analysis showed that unclassified Proteobacteria were also underrepresented in IL-22–neutralized HMA mice. It remains possible that these not-yet-

identified bacteria also play an important role in the protection against CDI. In addition to succinate, several other luminal metabolites were differentially abundant in control and IL-22–neutralized HMA mice, including taurocholate and taurine. Taurocholate is known to promote the germination of *C. difficile* spores [3], while microbiota-derived taurine is known to control microbial–host mutualism by modulating NLRP6-mediated anti-microbial peptide production by the intestinal epithelial cells [33]. Moreover, the concentration of various luminal amino acids was significantly increased in IL-22–neutralized HMA mice. As amino acid availability is closely associated with the risk for CDI [34], they may also contribute to the susceptible phenotype we observed in those mice. Consistent with these observations, the *Cd-CD2344*$^{-}$ strain, which cannot utilize succinate, was still able to proliferate in IL-22–neutralized HMA mice, although the early colonization of this strain was dramatically impaired compared to the WT strain. This result indicates that succinate is an important metabolite that promotes the proliferation of *C. difficile* in the gut early after its colonization. In later colonization, *C. difficile* may be able to use alternative nutritional sources, such as amino acids, for its growth. Thus, targeting different metabolic pathways, such as bile acid metabolism, succinate metabolism, and amino acid metabolism, by using multiple strains of commensal bacteria may be a more rational, and effective, strategy to prevent CDI.

Recent epidemiologic studies have shown that inflammatory bowel disease (IBD) patients, particularly UC, are at higher risk for CDI compared with non-IBD individuals [22, 23, 24]. Since CDI induces IBD flares and worsens disease outcome, CDI in IBD patients is recognized as a major clinical complication [22, 23, 24]. In the current study, we recapitulated increased susceptibility to CDI seen in UC patients using our HMA mouse model. Since it is known that the abundance of *Phascolarctobacterium* is decreased in IBD patients, both in UC and CD [35], the gut microbiotas derived from UC patients might have similar defects as those observed in IL-22–neutralized HMA mice, namely decreased abundance of *Phascolarctobacterium* and elevated levels of luminal succinate. Consistently, although the expression of IL-22 is up-regulated in the intestine of IBD patients [36, 37], there is evidence of possible defective IL-22 signaling in IBD, particularly UC, patients, such including the up-regulation of IL-22BP, which blocks IL-22 bioactivity [38, 39, 40, 41, 42, 43, 44]. Collectively, IL-22 signaling is likely compromised in UC patients. In this study, we discovered that the expression of IL-22BP (*IL22RA2*) is significantly up-regulated in UC patients, and that it inversely correlates with the expression of host glycosyltransferases, *MGAT4A* and *MGAT4B*. Reduced host *N*-glycosylation has been reported in active UC patients [45]. Our findings suggest that impaired IL-22 signaling in UC patients may cause abnormal host glycosylation, which triggers gut dysbiosis, including a reduction in the abundance of *Phascolarctobacterium* spp. Further study will be required to link IL-22 signaling, host glycosylation, and gut dysbiosis in patients with UC.

The increased luminal succinate level is likely only one facet of the complex process that increases the susceptibility of IBD patients to CDI. Indeed, FMT is much more effective than the administration of *Phascolarctobacterium* spp. to prevent CDI in UC-HMA mice, although *Phascolarctobacterium* spp. treatment significantly reduces the availability of luminal succinate. Consistently, FMT reduces the levels of various metabolites, such as amino acids, which are known to foster the growth of *C. difficile* [34]. It suggests that

Phascolarctobacterium spp. may be used with other bacterial strains that target distinct metabolic pathways related to *C. difficile* germination and growth (e.g., amino acid consumption, bile acid conversion) to improve clinical effectiveness further. In this regard, we are comparing the prevention efficacy of *Phascolarctobacterium* with that of a previously reported protective bacteria, such as *Clostridium scindens*, which resist to *C. difficile* in a secondary bile acid–dependent fashion [2]. We speculate that the combination of *Phascolarctobacterium* and *C. scindens* might have a synergistic effect in preventing CDI. However, further study is needed for developing a recipe of the effective cocktail of metabolic competitors that resists CDI. Although succinate may not be the only target for prevention of CDI in IBD patients, it remains possible that these parameters (i.e., the abundance of *Phascolarctobacterium*, the concentration of luminal succinate) could be used to screen and identify IBD patients who are at high risk for CDI. These findings also raise the question of whether modulation of IL-22 by current therapies for IBD could affect the incidence of *C. difficile* colitis.

Compared to CDI, clinical response to FMT in IBD is variable [46, 47]. This unresponsiveness of IBD patients to FMT might be, at least in part, due to insufficiencies of the nutritional niche caused by impaired host glycosylation. In this case, the combination of FMT and recombinant IL-22 (or co-inoculation with IL-22-inducing bacteria [48]) could maximize the colonization potential of transplanted beneficial bacteria, such as *Phascolarctobacterium* in the gut.

Our data clarify the role of IL-22 in the feedback regulation of the gut microbiota. IL-22-induced host glycosylation governs the growth of certain protective members of the gut microbiota, such as *Phascolarctobacterium*, and IL-22 normalizes the composition of the microbiota and influences its metabolic activities, which may be critical for the prevention of opportunistic colonization/expansion of *C. difficile* in the gut.

Methods

Mice

Specific pathogen-free (SPF) mice were housed in the Animal Facility at the University of Michigan. GF C57BL/6 and GF *Rag1*$^{-/-}$ mice were housed in the Germ-Free Animal Facility at the University of Michigan. GF mice were maintained in flexible film isolators and their GF status was checked weekly by aerobic and anaerobic culture. The absence of the microbiota was verified by microscopic analysis of stained cecal contents that detects any unculturable contamination. Histologically and endoscopically diagnosed UC patients and HC subjects were recruited through the University of Michigan IBD Databank (HUM0004184), and stool samples were collected from those donors. Individuals who received any antibiotics in the past 3 months were excluded. Individuals who had previous bacteria infections (e.g., *C. difficile*) or virus infections (e.g., hepatitis B virus, hepatitis C virus, or human immunodeficiency virus) were also excluded. Patient information was provided in Supplementary Table 5. Stool samples were resuspended in pre-reduced phosphate-buffered saline (in 1:10 ratio) in an anaerobic chamber and then filtrated through 100 μm cell strainer. Stool suspension was then inoculated into GF C57BL/6 mice or GF *Rag1*$^{-/-}$ mice (100 μl/mouse) [16].

Human microbiota-associated mice

The HMA mice were housed in positive-pressure individually ventilated cages (IVCs) (ISOcage P; Techniplast, West Chester, PA) in order to prevent cross-contamination and maintain their gnotobiotic status [49, 50]. All mice were fed a sterilized rodent breeder diet 5013 (LabDiet, St. Louis, MO). 8- to 16-week-old female and male mice were used in all experiments. All animals were handled in accordance with the protocols approved by the Institutional Animal Care and Use Committee (IACUC) at the University of Michigan. To attain robust *C. difficile* infection in HC-HMA mice, the animals were treated with a cocktail of antibiotics ofr 5 days. The cocktail contains kanamycin (0.4 mg/ml), gentamicin (0.035 mg/ml), colistin (850 U/ml), metronidazole, (0.215 mg/ml), and vancomycin (0.045 mg/ml). Clindamycin (10 mg/kg) was then injected intra-peritoneally at day 5. One day after clindamycin injection, mice were challenged by *C. difficile* 24 h post-IP injection [17].

Bacterial strain and *C. difficile* infection of mice

The spores of *C. difficile* strain VPI 10463 (ATCC 43255) were cultured at 65°C for 20 min at 65°C to kill vegetative bacteria. WT JIR8094 and *Cd-CD2344*$^{-}$ [21] were grown overnight in brain heart infusion medium supplemented with 100 mg/l L-cysteine and 5 mg/mL yeast extract (BHIS). Mice were infected with *C. difficile* VPI10463 spores (10^3 spores per mouse) or with an overnight culture of JIR8094/*Cd-CD2344*$^{-}$ (OD_{600} = 0.5–1.0, 200 μl per mouse) by oral gavage. Stool samples were collected from *C. difficile*–infected mice on days 1, 3, 7, 10, and 14 post-challenge. The samples were then serially diluted and plated on TCCFA selective plates to quantify the number of *C. difficile* spores under anaerobic conditions. For the αIL-22 antibody treatment, HC-HMA *Rag1*$^{-/-}$ mice were injected intraperitoneally twice before *C. difficile* inoculation (3 and 5 days prior to infection) and 3 times per week post-infection with the αIL-22 antibody (150 μg/mouse per dose) (Genentech, South San Francisco, CA, USA) or an equivalent amount of the isotype-matched control antibody (Genentech). For the IL-22-Fc fusion protein treatment, GF mice were injected intraperitoneally once before *Phascolaectobacterium* spp. (*P. faecium* JCM 30894 and *P. succinatutens* JCM 16074, 1×10^6 CFU each strain/mouse) inoculation (1 day prior to inoculation) and twice post inoculation (2 and 5 days) with IL-22-Fc (100 μg/mouse per dose) (Genentech) or an equivalent amount of the isotype-matched control protein (Genentech). For the succinate treatment, HC-HMA mice were given 1% succinate (Acros Organics, Belgium, WI) in drinking water 3 days prior to infection until sacrifice. *C. difficile*–infected UC-HMA mice were transplanted with a healthy human–derived microbiota (fecal microbiota transplantation; FMT) or *Phascolarctobacterium* (*P. faecium* JCM 30894 and *P. succinatutens* JCM 16074, 1×10^6 CFU each strain/mouse) once before *C. difficile* inoculation (3 days prior to infection) and 4 times post-inoculation (1, 3, 7, 10 days post-infection). Regarding the CDI experiments using SPF C57BL/6 mice, the mice were given cefoperazone (MP Biomedicals, Solon, OH) in drinking water (0.5 mg/mL) for 8 days, followed by regular water for 2 days. Then, the cefoperazone-treated SPF mice were infected with *C. difficile* VPI 10463 spores. For the prevention study, cefoperazone-treated SPF mice were inoculated with *P. faecium* JCM 30894 and *P. succinatutens* JCM 16074 (1×10^6 CFU each strain/mouse) once before *C. difficile* inoculation (3 days prior to infection) and 4 times post-inoculation (1, 3, 7, 10 days post-infection). HMA mice were sacrificed 7 days or 2 weeks post *C. difficile* inoculation. Cecum and colon tissues were collected and

fixed with 4% paraformaldehyde. Fixed tissues were then processed, embedded, sectioned and stained with hematoxylin and eosin (H&E). Histological inflammation was scored at the University of Michigan Unit for Laboratory Animal Medicine In-Vivo Animal Core. A veterinary pathologist evaluated histological inflammation in a blinded fashion. Histological scores were calculated based on following criteria: [1] Inflammation (0, none; 1, minimal multifocal inflammation [few foci]; 2, moderate multifocal inflammation [numerous foci]; 3, severe multifocal coalescing inflammation; and 4, same as a score of 3 with abscesses or extensive mural involvement); [2] edema (0, none; 1, mild focal or multifocal edema, minimal submucosal expansion (<2); 2, moderate focal or multifocal edema, moderate submucosal expansion (2–3); 3, severe multifocal to coalescing inflammation; and 4, same as a score of 3 with diffuse submucosal expansion); [3] epithelial damage (0, none; 1, mild, multifocal, superficial damage; 2, moderate, multifocal, superficial damage; 3, severe, multifocal to coalescing mucosal damage ± pseudomembrane ± ulcer; 4, same as a score of 3 with significant pseudomembrane or ulcer formation).

Quantitative Real-Time PCR

RNA was extracted with E.Z.N.A. Total RNA Kit (Omega Bio-tek, Norcross, GA) according to the manufacturer's instructions. RNA was reverse transcribed using a High Capacity RNA-to-cDNA Kit (Applied Biosystems, Foster, CA) and cDNA was then used for quantitative PCR analysis using SYBR Green Gene-Expression Assay on an ABI 7900HT analyzer (ABI 7900HT analyzer). The following primer sets were used for amplification: *Actb*-F; 5′-AAGTGTGACGTTGACATCCG, *Actb*-R; 5′-GATCCACATCTGCTGGAAGG, *Il22*-F; 5′-TTTCCTGACCAAACTCAGCA, *Il22*-R; 5′-TCTGGATGTTCTGGTCGTCA, *Reg3b* -F; 5′-CTCTCCTGCCTGATGCTCTT, *Reg3b* -R; 5′-GTAGGAGCCATAAGCCTGGG, *Reg3g*-F; 5′-TCAGGTGCAAGGTGAAGTTG, *Reg3g*-R; 5′-GGCCACTGTTACCACTGCTT, *GH73*-F; 5′-GCGTTTATGAAGTGCTGGAAAAG, *GH73*-R; 5′-ATTCCATACGCAGTTTCTCAGGT, *Mgat4a*-F; 5′-GCGACAGACAGAAGGCAAACC, *Mgat4a*-R; 5′-CCGACAGAGACGAGTGTAGGC, *Mgat4b*-F; 5′-AGGTGACGTGGTGGACATTT, *Mgat4b*-R; 5′-GCTTCAGGCTCTCTTGCTCA, *Mgat5*-F; 5′-GGAAATGGCCTTGAAAACACA, *Mgat5*-R; 5′-CAAGCACACCTGGGATCCA, *St6gal1*-F; 5′-TGCGTGTGGAAGAAAGGGAGC, *St6gal1*-R; 5′-CTCCTGGCTCTTCGGCATCTG, *Eubacteria*-F; 5′-ACTCCTACGGGAGGCAGCAGT, *Eubacteria*-R; 5′-ATTACCGCGGCTGCTGGC, *P. faecium*-F; 5′-CCTTTAGACGGGGACAACATTC, *P. faecium*-R; 5′-ATCGCCTTGGTAGTCCGTTACA, *P. succinatutens*-F; 5′-AGCAATCTCGCATGAGGATGCTGT, *P. succinatutens*-R; 5′-GCCGTGGCTTATTCGTTTACTACCG, mouse genomic Tnf (gTnf)−F; 5′-CAACCCTTATTCTCGCTCACA, gTnf−R; 5′-CTCCACACTCTCCTCCACCT, mouse genomic Actb (gActb)-F; 5' -ATGACCCAGATCATGTTTGA. mouse genomic Actb (gActb)-R; 5' TACGACCAGAGGGCATACAG

Microbiome analysis

Genomic DNA was extracted using a modified Qiagen DNeasy Blood and Tissue kit protocol (Qiagen, Valencia, CA) [16]. These modifications included the following steps: (1) UltraClean fecal DNA bead tubes (Mo Bio Laboratories, Inc, West Carlsbad, CA) and a

Mini-Beadbeater-16 (BioSpec Products, Inc, Bartlesville, OK) were used to homogenize samples (1.5 min); (2) the amount of buffer ATL used in the initial steps of the protocol was increased (from 180 to 400 μl); (3) the volume of proteinase K was increased (from 20 to 40 μl); and (4) the amount of buffer AE used to elute DNA at the end of the protocol was decreased (from 200 to 75 μl). The V4 region of bacterial 16S rRNA was sequenced using the Illumina MiSeq at the Host Microbiome Initiative University of Michigan. The sequence results were then analyzed by *Mothur* (v.1.33) [51, 52]. Operational taxonomic units (OTUs) (>97% identity) were curated and converted to relative abundance using *Mothur*. Shannon diversity index (H') and OUT richness were used to show community diversity. To compare the diversity between communities (β-diversity), we employed the Yue and Clayton (θ_{YC}) dissimilarity distance metric. θ_{YC} values were shown as non-metric multidimensional scaling (NMDS) plot. Linear discriminant analysis effect size (LEfSe) analysis was performed to identify differentially abundant taxa [53].

Metabolome analysis

The fecal samples for metabolome analysis were collected from HMA mice (2 weeks after inoculation with human stool sample) before CDI (at day 0). The fecal metabolomic profile was analyzed using capillary electrophoresis time-of-flight mass spectrometry (CE-TOFMS) [54]. Lyophilized fecal samples were homogenized by a Shake Master (Biomedical Science, Tokyo, Japan) with 3.0-mm Zirconia Beads (Biomedical Science, Tokyo, Japan). Homogenized fecal samples were then resuspended in methanol:chloroform:water solution to extract metabolites. The Agilent CE System, the Agilent G3250AA LC/MSD TOF System, the Agilent 1100 Series Binary HPLC Pump, the G1603A Agilent CE-MS adapter, and the G1607A Agilent CE-ESI-MS Sprayer Kit (Agilent Technologies, Santa Clara, CA) were used for CE-TOFMS analysis. Data are processed by the MasterHands software. For luminal succinate analysis, frozen stool samples were analyzed using liquid chromatography–mass spectrometry (LC-MS) at the Michigan Regional Comprehensive Metabolomics Resource Core [55]. In brief, fecal samples were resuspended in 0.5 ml of extraction solution (methanol: chloroform: water = 8:1:1) containing ^{13}C4-labeled succinate. The samples were then homogenized and incubated at 4°C for 10 min. The extract was harvested by centrifuging suspension at 4°C, 14,000 rpm for 10 min. An A 1260 UPLC module coupled with a 6520 quadrupole time-of-flight (Q-TOF) mass spectrometer (Agilent Technologies, Santa Clara, CA.) was used for LC-MS analysis. A 150 × 1 mm Luna NH_2 hydrophilic interaction chromatography column (Phenomenex, Torrance, CA) was used to separate metabolites. MassHunter Quantitative Analysis Reporting B.07.00 Service Pack (Agilent Technologies) was used for data processing. Succinate was normalized to its isotopically labeled internal standard and quantitated using 2 replicated injections of 5 standards to create a linear calibration curve with accuracy better than 80% for each standard. Other compounds in the analysis were normalized to the nearest internal standard, and the peak areas were used for differential analysis between groups.

Ex vivo growth of *C. difficile* (JIR8094 and *Cd-CD2344*$^{-}$)

Overnight cultures of JIR8094 and *Cd-CD2344*$^{-}$ were diluted 5000-fold with a minimal medium (10 g/l peptone, 10 g/l beef extract, 3 g/l yeast extract, 1.55 g/l $NaH_2PO_4 \cdot H_2O$, 5.95 g/l Na_2HPO_4) supplemented with 1% glucose, 0.1% succinate, or 100 μg/mL UC luminal

content. A handheld spectrophotometer (Biochrom US, Holliston, MA) was used for optical density (OD_{600}) measurements.

Ex vivo germination and growth of *C. difficile* (VPI10463)

Mouse cecal contents from HC-HMA and UC-HMA mice were quantified inside an anaerobic chamber and diluted 10-fold with PBS. Heat-treated (65°C, 20 min) *C. difficile* spores (10^3 spores) were added to the cecal contents, which were then incubated anaerobically at 37°C for 6 h. After incubation, bacterial samples were serially diluted, plated on TCCFA plates in order to quantify germination and growth of *C. difficile* [3].

In vitro growth of *Phascolarctobacterium*

P. faecium JCM 30894 and *P. succinatutens* JCM 16074 (JCM, Ibaragi, Japan) were grown overnight in a peptone yeast extract medium supplemented with 80 mM sodium succinate (PYS) under anaerobic conditions [19]. The overnight culture of *Phascolarctobacterium* spp. was diluted 100-fold with PYS medium. In some experiments, 100 mM GlcNAc (MilliporeSigma, St. Louis, MO) was added. For the growth assay on mucus medium, SPF WT C57BL/6 mice (some, but not all mice were littermates) were co-housed for over 2 weeks, and then randomly separated into two groups. One group was treated with αIL-22 antibody and the other with the control antibody. Colonic mucus was scraped from colonic walls into HEPES-Hank's buffer (8.0 g/Ll NaCl, 0.4 g/l KCl, 0.05 g/l $CaCl_2$•H_2O, 0.35 g/l KH_2PO_4, 0.2 g/l $MgSO_4$ • $7H_2O$, and 2.6 g/l HEPES, pH 7.4). Contaminating epithelial cells and membranes were removed by centrifugation, once at 12,000 g for 10 min, and once at 27,000 *g* for 15 min at 4°C. Colonic mucus in HEPES-Hank's buffer was stored at −80°C until further use [56]. 300 μg of colonic mucus scrape from the control and the αIL-22 antibody–treated mice were added to the PYS medium. *Phascolarctobacterium* spp. were cultured anaerobically for 24–48 h. Bacterial RNAs were purified and GH family gene expression was quantified by qPCR. The CFU count was determined by culturing samples on PYS agar plates.

Glycan analysis

The mucus samples were scraped from the colonic tissues. The scraped mucus was suspended in GuHCl buffer (6 M GuHCl, 5 mM EDTA, 10 mM NaH_2PO_4, and 5 mM PMSF), on a rolling wheel, in a cold room, overnight. The samples were separated into a soluble fraction (supernatant) and an insoluble fraction (pellet) by centrifugation at full speed for 10 min at 4°C. The insoluble fraction was solubilized by adding 0.975 mL solubilization buffer (6 M GuHCl, 100 mM Tris, 5 mM DETA) along with 25 mM DTT and 5 mM PMSF. The solution was kept on a rolling wheel overnight in a cold room. After incubation, iodoacetamide was added, and the solution was incubated in the dark for 4 h at room temperature. The pellet was removed by centrifugation at full speed for 10 min at 4°C. Both soluble and insoluble fractions were transferred to a PVDF membrane using dot-blotting. The membrane was stained with Alcian blue, followed by destaining with methanol. *N*- and *O*-linked oligosaccharides were released from glycoproteins blotted on PVDF membranes for glycan analysis [57]. The *N*-glycans were first released from the PVDF membrane. The membrane was blocked with 1% PVP solution (polyvinyl pyrrolidone 40,000, w/w) in 50% methanol and then washed 3 times in water and shaken for 5 min.

Next, the membrane was added 50 mM NH_4Ac (pH 8.4) and PNGase. After overnight incubation at 37°C, the sample was dried using SpeedVac. The left membrane dots were subjected to *O*-glycans release. The *N*-glycans were reduced by incubating with 20 mM NaOH and 0.5 M $NaBH_4$ overnight at 50°C. The salt was removed as *O*-glycans. The *O*-glycans on the dot blots were released by reducing beta-elimination and desalted. Released *O*-glycans were resuspended in water and analyzed by liquid chromatography–electrospray ionization tandem mass spectrometry (LC-ESI/MS). A 5 μm porous graphite particles column (Hypercarb, Thermo-Hypersil, Runcorn, UK) was used to separate oligosaccharides. The loaded oligosaccharides were eluted with 0%−45% gradient of Buffer B (10 mM ammonium bicarbonate in 80% acetonitrile) followed by a wash step with 100% Buffer B. The column was then equilibrated with Buffer A (10 mM ammonium bicarbonate). An LTQ linear ion trap mass spectrometer (Thermo Electron, San Jose, CA) in negative ion mode was used to analyze the samples. Xcalibur software (Version 2.0.7) was used for data acquisition and analysis.

The Gene Expression Omnibus (GEO) accession number

Publicly available gene expression data used in this study are available from the NCBI Gene Expression Omnibus under the following accession codes: GSE75214 [25], GSE16879 [26], and GSE73661 [27].

Statistical Analyses

Statistical analyses were performed using GraphPad Prism software version 6.0 (GraphPad Software Inc.). Statistical tests used for the analysis of data are identified in the legend of each figure. Differences of $P < 0.05$ were considered significant.

Extended Data

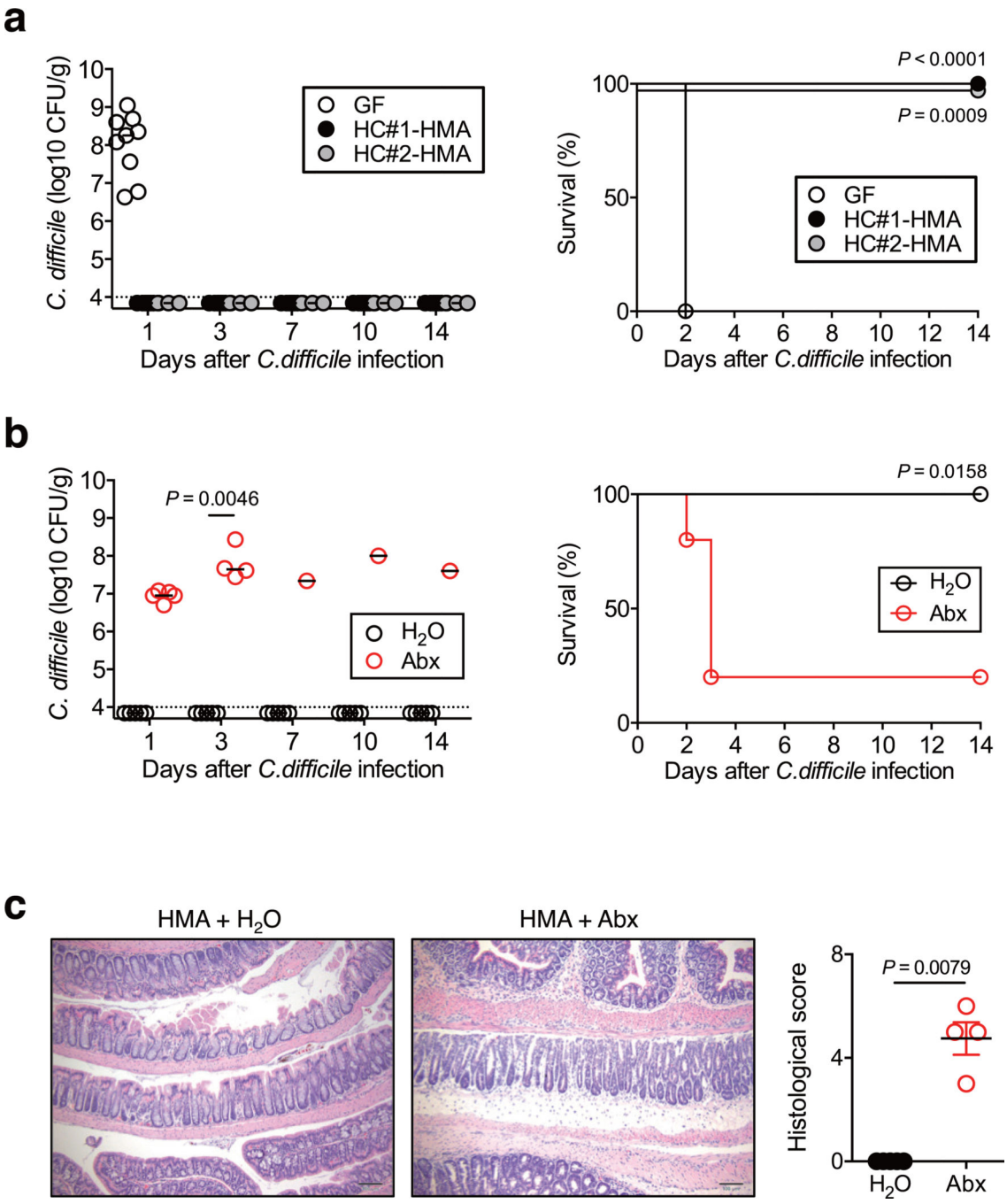

Extended Data Fig. 1. Healthy human microbiotas prevent *C. difficile* infection.

(**a**) (Left) GF B6 mice were colonized with healthy control (HC) microbiotas for 2 weeks (human microbiota-associated (HMA) mice). GF or HC-HMA mice (GF: n=9, HC#1:n=8 and HC#2:n=3, biologically independent animals) were then infected with *C. difficile* VPI 10463 spores (10^3 spores/mouse). *C. difficile* load in feces was determined on indicated days post-infection. Dots represent individual mice. Bars indicate median. Data were pooled from 2 independent experiments. (Right) The mortality of *C. difficile* infected GF or HC-HMA mice. Statistical significance was assessed by Log-rank test (two-sided). (**b** and **c**) (**b**) HC-

HMA mice were treated with a cocktail of antibiotics or regular water and then infected with *C. difficile* VPI 10463 spores (n=5, biologically independent animals). (Left) CFU in feces. Dots represent individual mice. Bars indicate median. Data were pooled from 2 independent experiments. Statistical significance was assessed by 2-way ANOVA with Bonferroni post-hoc test (two-sided). (Right) The mortality of mice. Statistical significance was assessed by Log-rank test (two-sided). (**c**) Representative histological images and associated histological scores. Scale bar is 100 μm. Data are presented as mean ± s.e.m. from pooled two independent experiments. Statistical significance was assessed by Mann-Whitney *U* test (two-sided).

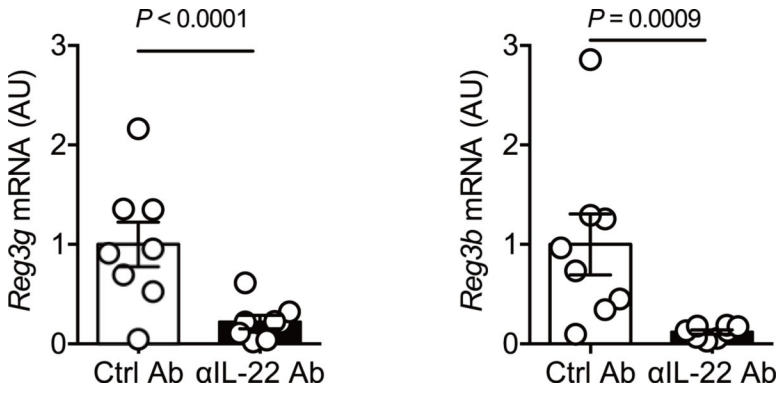

Extended Data Fig. 2. IL-22 neutralization inhibits the expression of antimicrobial proteins.

Reg3b and *Reg3g* mRNA levels in control or αIL-22 antibody-treated HC-HMA *Rag1*$^{-/-}$ mice were determined by qPCR. Expression was normalized to that of the murine *Actb* gene. Dots represent individual mice. Data are presented as mean ± s.e.m. (n=8, biologically independent animals) from pooled 2 independent experiments. Statistical significance was assessed by Mann-Whitney *U* test (two-sided).

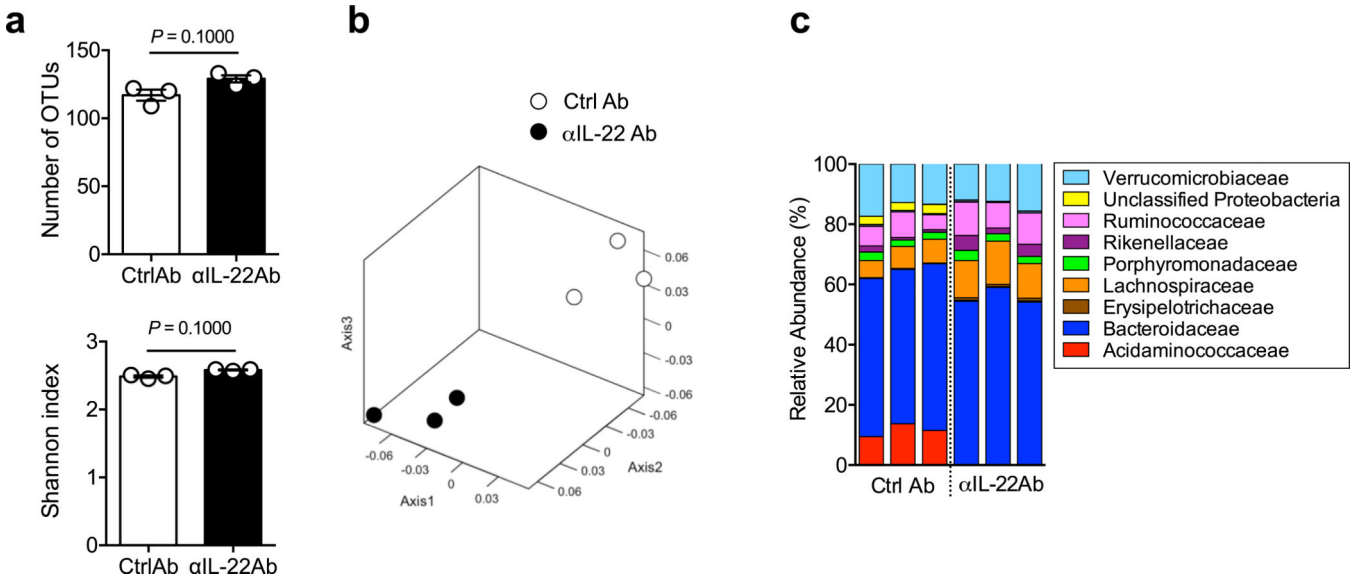

Extended Data Fig. 3. IL-22 shapes the gut microbial community.

HC-HMA-*Rag1*$^{-/-}$ mice were treated with control or αIL-22 antibody twice, on day −5 and day −3, before fecal samples were collected. Bacterial 16S rRNA sequences were analyzed. (**a**) Shannon index (α-diversity) and number of OTUs (richness) of control and αIL-22 antibody-treated HMA-*Rag1*$^{-/-}$ mice. Dots represent individual mice. Data are presented as mean ± s.e.m. (n=3, biologically independent animals). Data are representative of 2 independent experiments. Statistical significance was assessed by Mann-Whitney *U* test (two-sided). (**b**) Microbial community structures were analyzed using the Yue and Clayton dissimilarity distance metric (θ_{YC}) and are shown in a nonmetric, multidimensional scaling plot. (**c**) Bacterial taxonomy at the family level in the feces.

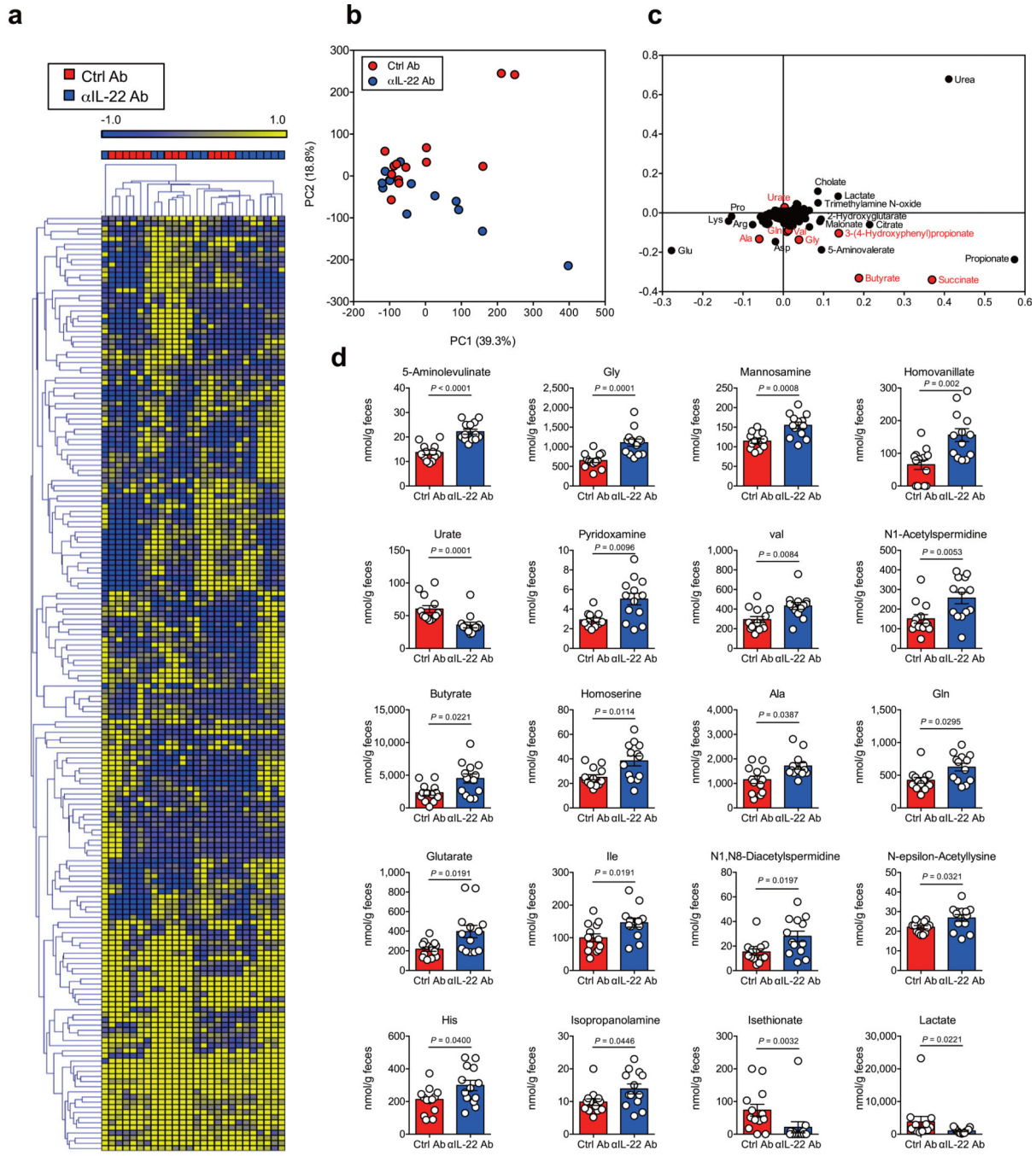

Extended Data Fig. 4. Luminal metabolomic analysis in IL-22–neutralized HMA mice.

(**a**) Fecal samples were collected after treatment with αIL-22 antibody, twice and before CDI (day 0). A heat map showing the quantified metabolic profiles of control or αIL-22 antibody-treated HC-HMA-*Rag1*$^{-/-}$ mice. All concentrations of quantified metabolites were transformed into Z-scores and clustered according to their Euclidean distance. Gray areas in the heat map indicate that respective metabolites were not detected. (**b**) Principal component analysis of the metabolome data. (**C**) A loading scatter plot of the principal component analysis. (**d**) Luminal metabolites were analyzed by CE-TOF/MS. Dots represent individual

mice. Data are presented as mean ± s.e.m. (n=13, biologically independent animals) from pooled 3 independent experiments. Statistical significance was assessed by Mann-Whitney *U* test (two-sided).

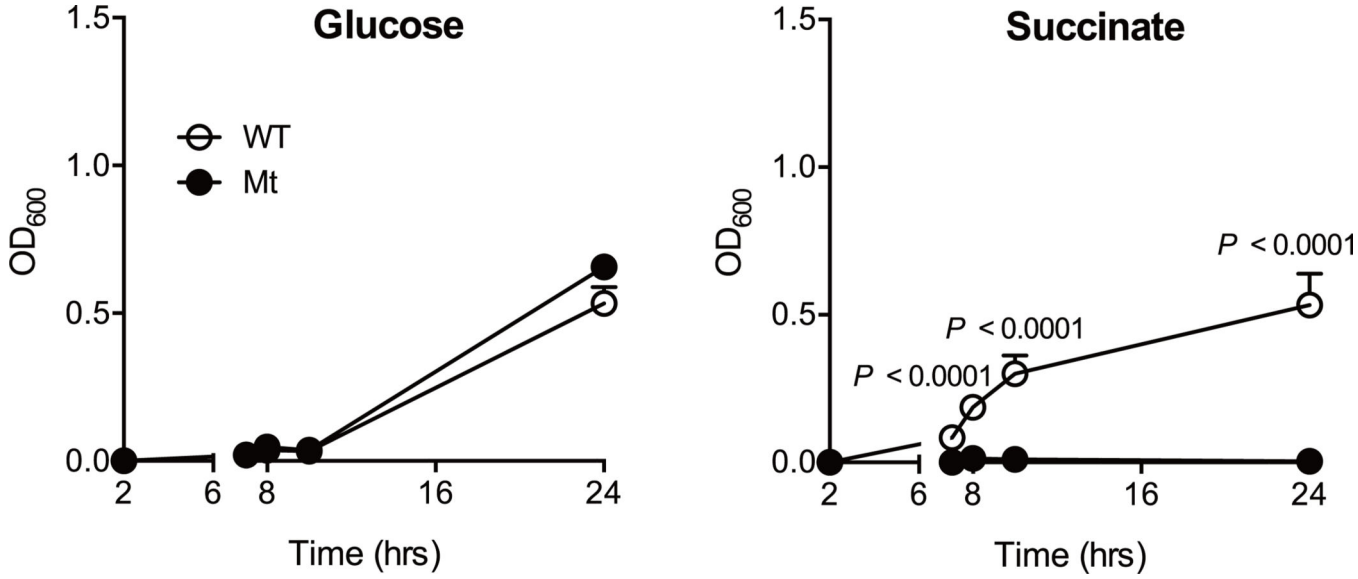

Extended Data Fig. 5. *C. difficile* growth on succinate.

In vitro growth of WT JIR8094 or *Cd-CD2344-* mutant *C. difficile* in a minimal medium supplemented with glucose or succinate. Data are presented as mean ± s.d. (n=3 technical replicates). Data are representative of 3 independent experiments. Statistical significance was assessed by 2-way ANOVA with Bonferroni post-hoc test (two-sided).

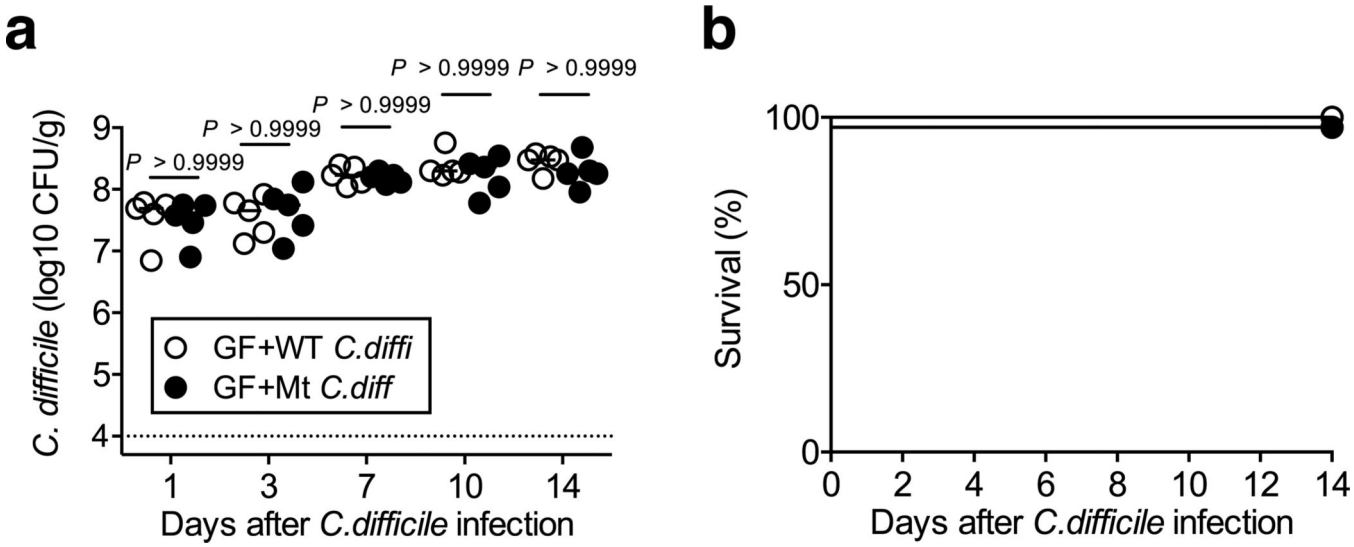

Extended Data Fig. 6. Succinate is not required for the growth of *C. difficile* in germ-free mice.
GF C57BL/6 mice were infected with WT JIR8094 or *Cd-CD2344*¯ mutant *C. difficile* strains. *C. difficile* load in feces was determined on indicated days post-infection (n=5, biologically independent animals). Dots represent individual mice. Bars indicate median. Data were from pooled 2 independent experiments. Statistical significance was assessed by 2-way ANOVA with Bonferroni post-hoc test (two-sided).

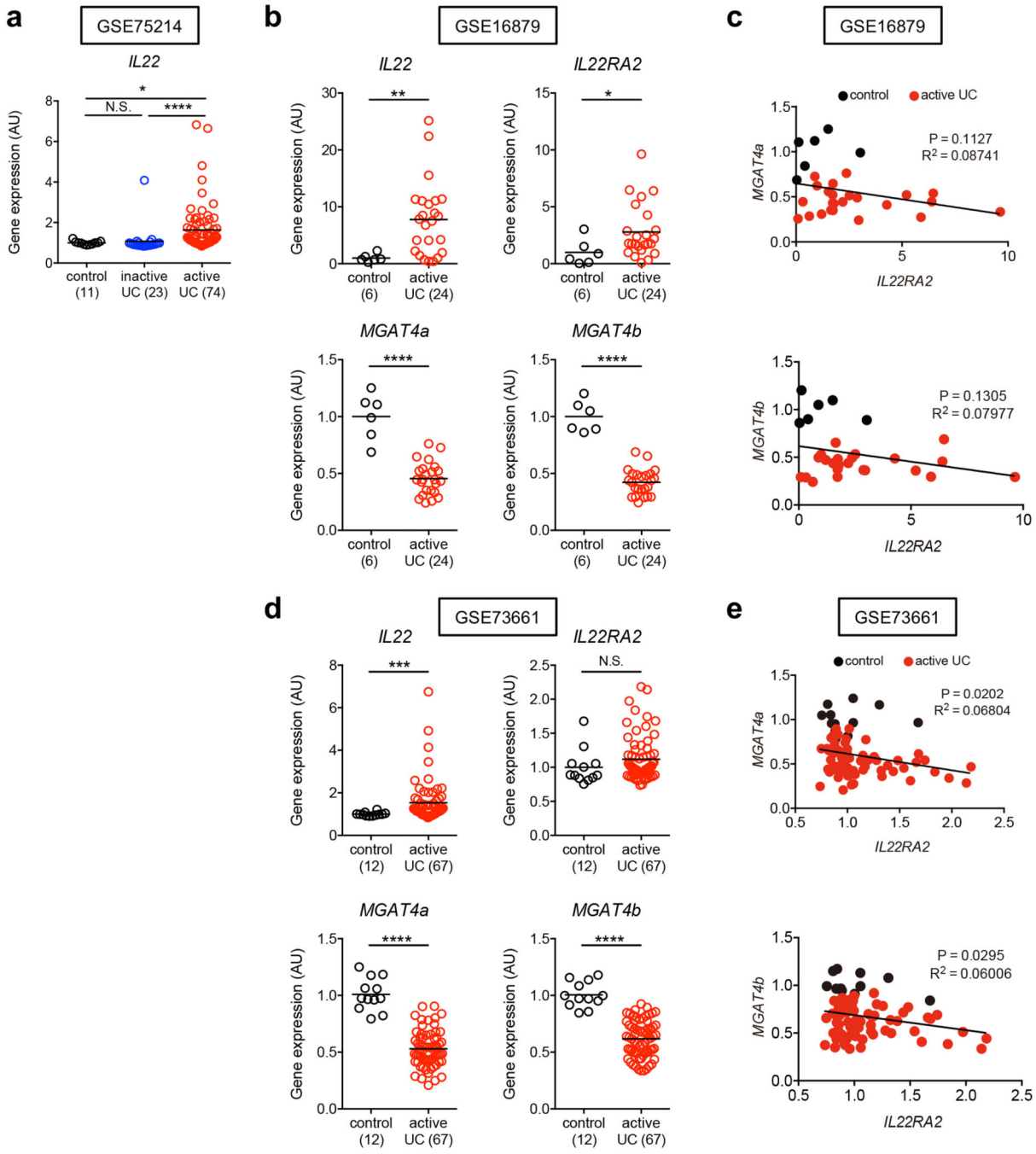

Extended Data Fig. 7. Gene expression profiles in UC patient cohorts.

(**a**) The mRNA expression of *IL22* mRNA in the colonic tissue from control subjects (n=11), patients with inactive UC (n=23) and patients with active UC (n=74). Data were derived from GEO data set GSE75214. Dots represent biologically independent subjects. Data are presented as mean ± s.e.m.. Statistical significance was assessed by Kruskal-Wallis test with Dunn posttest (two-sided). (**b** and **d**) The mRNA expression of *IL22, IL22RA, MGAT4A* and *MGAT4B* mRNA in the colonic tissue from control subjects and patients with active UC. (**c** and **e**) Correlation between *MGAT4A*/*MGAT4B* and *IL22RA* mRNA expression in 3

groups. Statistical significance was measured by Pearson correlation test (two-sided). Dots represent biologically independent subjects. Data were derived from GEO data sets GSE16879 (control: n=8 and active UC: n=24) and GSE73661 (control: n=12 and active UC: n=67). Data are presented as mean ± s.e.m.. Statistical significance was assessed by Mann-Whitney *U* test (two-sided). (**b** and **d**). Statistical significance was measured by Pearson correlation test (two-sided) (**c** and **e**).

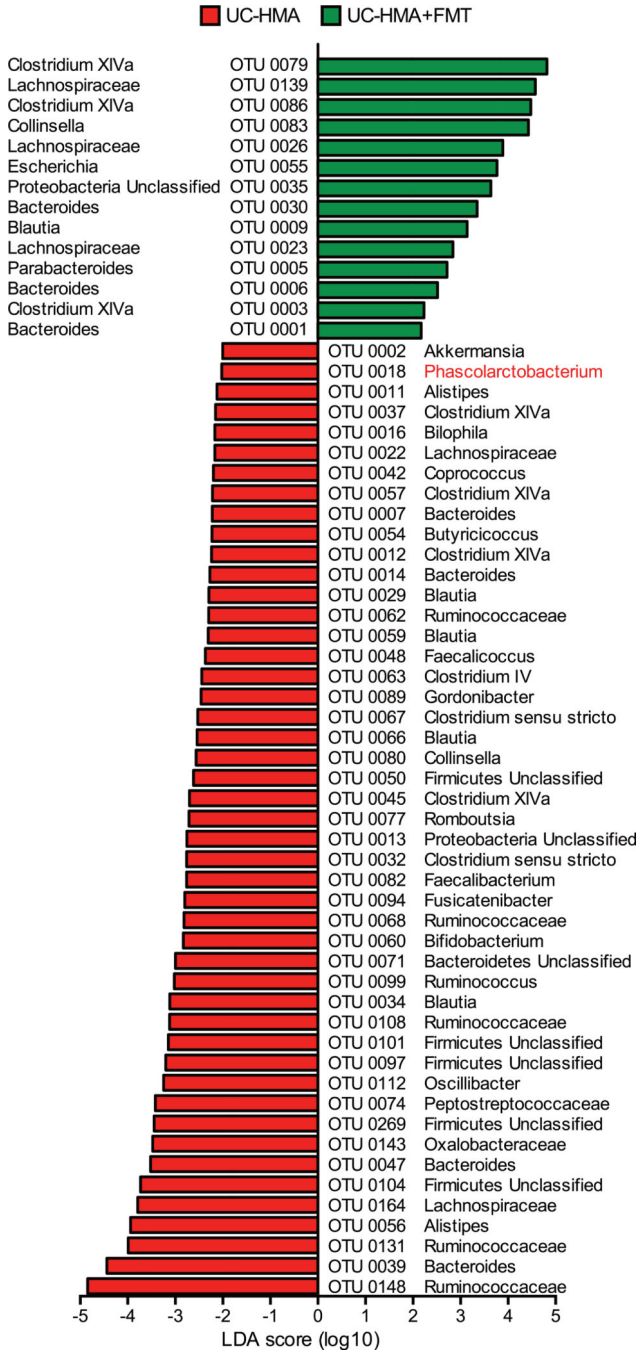

Extended Data Fig. 8. FMT restores the microbial composition in UC-HMA mice.

Significantly altered bacteria in pre–*C. difficile* infected UC-HMA mice with or without FMT were identified by LEfSe analysis. UC-HMA mice–enriched taxa have a positive LDA score (red, n=6, biologically independent animals), and FMT-treated UC-HMA mice–enriched taxa have a negative LDA score (green, n=6, biologically independent animals). A *P* value of < 0.05 and a score ≥ 2.0 were considered significant in Kruskal–Wallis and pairwise Wilcoxon tests (two-sided), respectively.

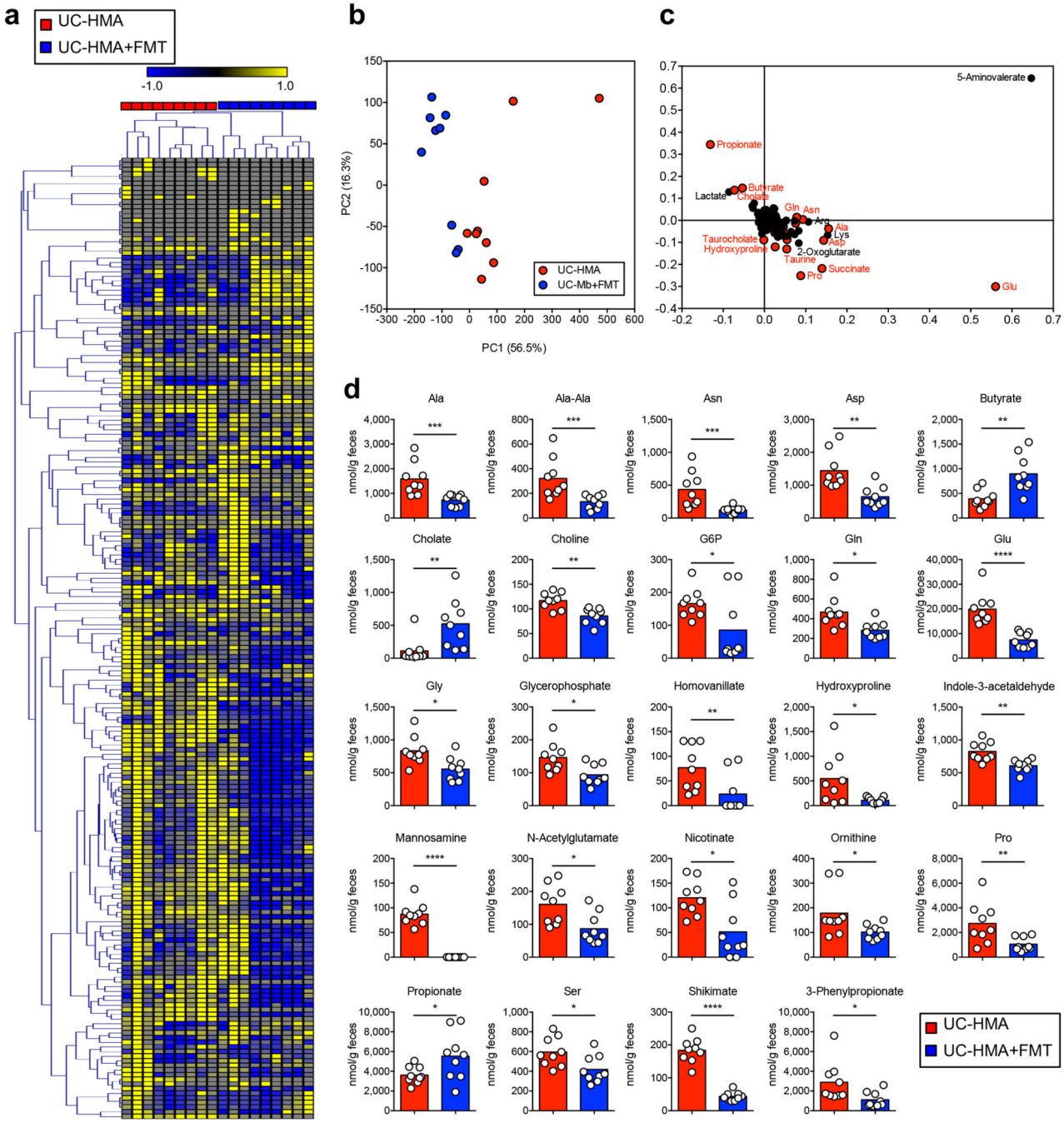

Extended Data Fig. 9. Luminal metabolomic analysis in FMT-treated UC-HMA mice.

(**a**) Fecal samples were collected after treatment with FMT (day −3) and before CDI (day 0). A heat map showing the quantified metabolic profiles of UC-HMA or FMT-treated UC-HMA mice. All concentrations of quantified metabolites were transformed into Z-scores and clustered according to their Euclidean distance. Gray areas in the heat map indicate that respective metabolites were not detected. (**b**) The principal component analysis of the metabolome data (n=9, biologically independent animals). (**C**) A loading scatter plot of the principal component analysis. (**d**) Luminal metabolites were analyzed by CE-TOF/MS. Dots

represent individual mice. Data are presented as mean ± s.e.m. (n=9, biologically independent animals) from pooled 2 independent experiments. Statistical significance was assessed by Mann-Whitney *U* test (two-sided).

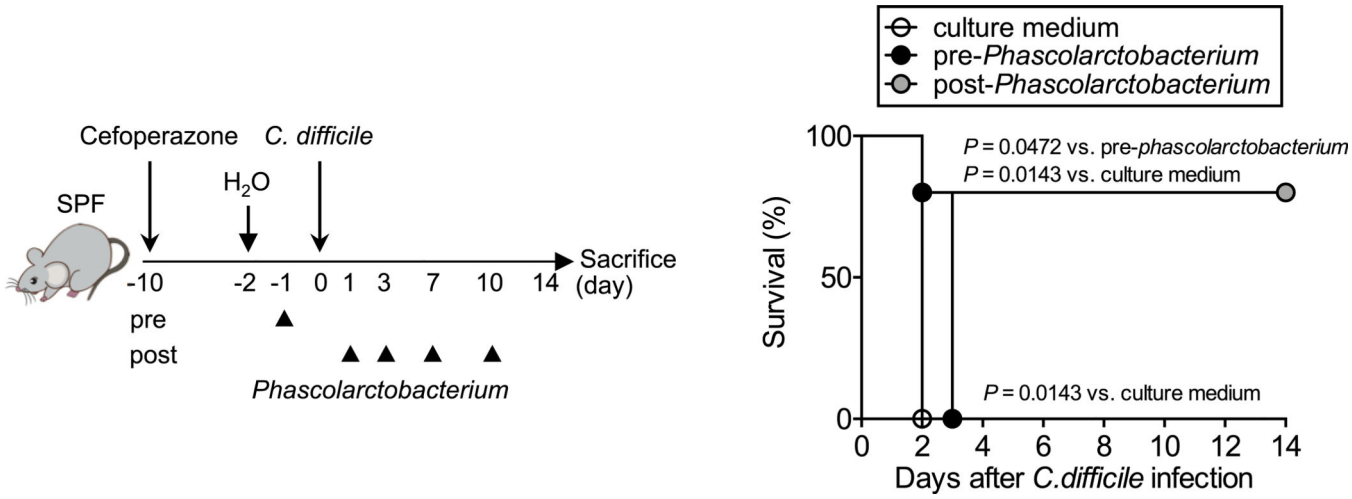

Extended Data Fig. 10. *Phascolarctobacterium* inoculation protect mice from CDI.

SPF C57BL/6 mice were treated with cefoperazone (0.5 mg/mL in drinking water). After 8 days, the mice were switched to regular water and allowed to recover for 2 days before being infected with *C. difficile* VPI spores. Mice were treated with *P. faecium* JCM 30894 and *P. succinatutens* JCM 16074 (10^6 CFU each strain) or with its culture medium by oral gavage, once, before *C. difficile* inoculation (1 day prior to CDI, pre-treatment) or 4 times post-inoculation (1, 3, 7, 10 days post-infection, post-treatment). Dots represent individual mice (n=5, biologically independent animals). The mortality of *C. difficile*–infected mice was assessed. Statistical significance was assessed by Log-rank test (two-sided) from pooled 2 independent experiments.

Supplementary Material

Refer to Web version on PubMed Central for supplementary material.

Acknowledgments

The authors thank Andrew B. Shreiner for technical assistance, the University of Michigan Center for Gastrointestinal Research (UMCGR) (DK034933), Host Microbiome Initiative, the Germ-free Animal Facility, the Michigan Regional Comprehensive Metabolomics Resource Core (MRC2) (DK097153) for core services, and Ingrid L. Bergin from the In-Vivo Animal Core at the University of Michigan Unit for Laboratory Animal Medicine for histological assessment. This work was supported by National Institute of Health DK110146 and DK108901 (N.K.), Crohn's and Colitis Foundation of America (N. K and H. N.-K.), Young Investigator Grant from the Global Probiotics Council (N.K.), University of Michigan Center for Gastrointestinal Research DK034933 (N. K.), Joint Usage/Research Program of Medical Mycology Research Center Chiba University 18–1 (N.K. and Y.G.), JSPS Postdoctoral Fellowship for Research Abroad (H. N.-K. and S.K.), the Uehara Memorial Foundation Postdoctoral Fellowship Award (S.K.), Clinical and Translational Science Awards (CTSA) Program (S.K.), and Prevent Cancer Foundation (S.K.). JSPS KAKENHI 16H04901, 17H05654, 18H04805 (S.F.), PRESTO JPMJPR1537 (S.F.), JST ERATO JPMJER1902 (S.F.), AMED-CREST JP19gm1010009 (S.F.), the Takeda Science Foundation (S.F.), the Food Science Institute Foundation (S.F.). MS analysis of glycans was performed by the Swedish infrastructure for biological mass spectrometry (BioMS) supported by the Swedish Resarch Council.

Data Availability:

Source data for all Figures and Extended data Figures are provided with the paper. The microbiome data in this study is available at the National Center for Biotechnology Information (NCBI) Sequence Read Archive under BioProject PRJNA594915. The metabolome data is available at the NIH Common Fund's Data Repository and Coordinating Center (supported by NIH grant, U01-DK097430) website, the Metabolomics Workbench, http://www.metabolomicsworkbench.org, where it has been assigned Project ID PR000882 (αIL-22 Ab experiment in

Fig. 2b and Extended Data Fig. 4), PR000881 (FMT experiment in Fig. 6f and Extended Data Fig. 9), and PR000869 (*Phascolarctobacterium* administration in Fig. 6i).

References

1. Britton RA & Young VB Role of the intestinal microbiota in resistance to colonization by Clostridium difficile. Gastroenterology 146, 1547–1553 (2014). [PubMed: 24503131]
2. Buffie CG et al. Precision microbiome reconstitution restores bile acid mediated resistance to Clostridium difficile. Nature 517, 205–208 (2015). [PubMed: 25337874]
3. Theriot CM et al. Antibiotic-induced shifts in the mouse gut microbiome and metabolome increase susceptibility to Clostridium difficile infection. Nat Commun 5, 3114 (2014). [PubMed: 24445449]
4. Kamada N & Nunez G Role of the gut microbiota in the development and function of lymphoid cells. J Immunol 190, 1389–1395 (2013). [PubMed: 23378581]
5. Sonnenberg GF et al. Innate lymphoid cells promote anatomical containment of lymphoid-resident commensal bacteria. Science 336, 1321–1325 (2012). [PubMed: 22674331]
6. Zheng Y et al. Interleukin-22 mediates early host defense against attaching and effacing bacterial pathogens. Nat Med 14, 282–289 (2008). [PubMed: 18264109]
7. Sakamoto K et al. IL-22 Controls Iron-Dependent Nutritional Immunity Against Systemic Bacterial Infections. Science immunology 2 (2017).
8. Pham TA et al. Epithelial IL-22RA1-mediated fucosylation promotes intestinal colonization resistance to an opportunistic pathogen. Cell Host Microbe 16, 504–516 (2014). [PubMed: 25263220]
9. Pickard JM et al. Rapid fucosylation of intestinal epithelium sustains host-commensal symbiosis in sickness. Nature 514, 638–641 (2014). [PubMed: 25274297]
10. Goto Y et al. Innate lymphoid cells regulate intestinal epithelial cell glycosylation. Science 345, 1254009 (2014). [PubMed: 25214634]
11. Satoh-Takayama N et al. Microbial flora drives interleukin 22 production in intestinal NKp46+ cells that provide innate mucosal immune defense. Immunity 29, 958–970 (2008). [PubMed: 19084435]
12. Sanos SL et al. RORgammat and commensal microflora are required for the differentiation of mucosal interleukin 22-producing NKp46+ cells. Nat Immunol 10, 83–91 (2009). [PubMed: 19029903]
13. Sadighi Akha AA et al. Interleukin-22 and CD160 play additive roles in the host mucosal response to Clostridium difficile infection in mice. Immunology 144, 587–597 (2015). [PubMed: 25327211]
14. Hasegawa M et al. Interleukin-22 regulates the complement system to promote resistance against pathobionts after pathogen-induced intestinal damage. Immunity 41, 620–632 (2014). [PubMed: 25367575]
15. Abt MC et al. Innate Immune Defenses Mediated by Two ILC Subsets Are Critical for Protection against Acute Clostridium difficile Infection. Cell Host Microbe 18, 27–37 (2015). [PubMed: 26159718]
16. Nagao-Kitamoto H et al. Functional characterization of inflammatory bowel disease-associated gut dydbiosis in gnotobiotic mice. Cellular and Molecular Gastroenterology and Hepatology 2, 468–481 (2016). [PubMed: 27795980]
17. Collins J, Auchtung JM, Schaefer L, Eaton KA & Britton RA Humanized microbiota mice as a model of recurrent Clostridium difficile disease. Microbiome 3, 35 (2015). [PubMed: 26289776]
18. Sonnenberg GF & Artis D Innate lymphoid cell interactions with microbiota: implications for intestinal health and disease. Immunity 37, 601–610 (2012). [PubMed: 23084357]
19. Watanabe Y, Nagai F & Morotomi M Characterization of Phascolarctobacterium succinatutens sp. nov., an asaccharolytic, succinate-utilizing bacterium isolated from human feces. Appl Environ Microbiol 78, 511–518 (2012). [PubMed: 22081579]
20. Topping DL & Clifton PM Short-chain fatty acids and human colonic function: roles of resistant starch and nonstarch polysaccharides. Physiological reviews 81, 1031–1064 (2001). [PubMed: 11427691]

21. Ferreyra JA et al. Gut microbiota-produced succinate promotes C. difficile infection after antibiotic treatment or motility disturbance. Cell Host Microbe 16, 770–777 (2014). [PubMed: 25498344]
22. Rodemann JF, Dubberke ER, Reske KA, Seo da H & Stone CD Incidence of Clostridium difficile infection in inflammatory bowel disease. Clin Gastroenterol Hepatol 5, 339–344 (2007). [PubMed: 17368233]
23. Reddy SS & Brandt LJ Clostridium difficile infection and inflammatory bowel disease. J Clin Gastroenterol 47, 666–671 (2013). [PubMed: 23507767]
24. Berg AM, Kelly CP & Farraye FA Clostridium difficile infection in the inflammatory bowel disease patient. Inflamm Bowel Dis 19, 194–204 (2013). [PubMed: 22508484]
25. Vancamelbeke M et al. Genetic and Transcriptomic Bases of Intestinal Epithelial Barrier Dysfunction in Inflammatory Bowel Disease. Inflamm Bowel Dis 23, 1718–1729 (2017). [PubMed: 28885228]
26. Arijs I et al. Mucosal gene expression of antimicrobial peptides in inflammatory bowel disease before and after first infliximab treatment. PLoS One 4, e7984 (2009). [PubMed: 19956723]
27. Arijs I et al. Effect of vedolizumab (anti-alpha4beta7-integrin) therapy on histological healing and mucosal gene expression in patients with UC. Gut 67, 43–52 (2018). [PubMed: 27802155]
28. Johnson JL, Jones MB, Ryan SO & Cobb BA The regulatory power of glycans and their binding partners in immunity. Trends Immunol 34, 290–298 (2013). [PubMed: 23485517]
29. Stanley P What Have We Learned from Glycosyltransferase Knockouts in Mice? Journal of molecular biology 428, 3166–3182 (2016). [PubMed: 27040397]
30. Wu F et al. Phascolarctobacterium faecium abundant colonization in human gastrointestinal tract. Experimental and therapeutic medicine 14, 3122–3126 (2017). [PubMed: 28912861]
31. Zhang L et al. Insight into alteration of gut microbiota in Clostridium difficile infection and asymptomatic C. difficile colonization. Anaerobe 34, 1–7 (2015). [PubMed: 25817005]
32. Hourigan SK et al. Microbiome changes associated with sustained eradication of Clostridium difficile after single faecal microbiota transplantation in children with and without inflammatory bowel disease. Aliment Pharmacol Ther 42, 741–752 (2015). [PubMed: 26198180]
33. Levy M et al. Microbiota-Modulated Metabolites Shape the Intestinal Microenvironment by Regulating NLRP6 Inflammasome Signaling. Cell 163, 1428–1443 (2015). [PubMed: 26638072]
34. Battaglioli EJ et al. Clostridioides difficile uses amino acids associated with gut microbial dysbiosis in a subset of patients with diarrhea. Sci Transl Med 10 (2018).
35. Morgan XC et al. Dysfunction of the intestinal microbiome in inflammatory bowel disease and treatment. Genome Biol 13, R79 (2012). [PubMed: 23013615]
36. Wolk K et al. IL-22 induces lipopolysaccharide-binding protein in hepatocytes: a potential systemic role of IL-22 in Crohn's disease. J Immunol 178, 5973–5981 (2007). [PubMed: 17442982]
37. Schmechel S et al. Linking genetic susceptibility to Crohn's disease with Th17 cell function: IL-22 serum levels are increased in Crohn's disease and correlate with disease activity and IL23R genotype status. Inflamm Bowel Dis 14, 204–212 (2008). [PubMed: 18022867]
38. Mann ER et al. Human gut dendritic cells drive aberrant gut-specific t-cell responses in ulcerative colitis, characterized by increased IL-4 production and loss of IL-22 and IFNgamma. Inflamm Bowel Dis 20, 2299–2307 (2014). [PubMed: 25397892]
39. Leung JM et al. IL-22-producing CD4+ cells are depleted in actively inflamed colitis tissue. Mucosal Immunol 7, 124–133 (2014). [PubMed: 23695510]
40. Lamas B et al. CARD9 impacts colitis by altering gut microbiota metabolism of tryptophan into aryl hydrocarbon receptor ligands. Nat Med 22, 598–605 (2016). [PubMed: 27158904]
41. Martin JC et al. IL-22BP is produced by eosinophils in human gut and blocks IL-22 protective actions during colitis. Mucosal Immunol 9, 539–549 (2016). [PubMed: 26329427]
42. Pelczar P et al. A pathogenic role for T cell-derived IL-22BP in inflammatory bowel disease. Science 354, 358–362 (2016). [PubMed: 27846573]
43. Xu AT et al. High suppressor of cytokine signaling-3 expression impairs STAT3-dependent protective effects of interleukin-22 in ulcerative colitis in remission. Inflamm Bowel Dis 21, 241–250 (2015). [PubMed: 25545374]

44. Li Y et al. Increased suppressor of cytokine signaling-3 expression predicts mucosal relapse in ulcerative colitis. Inflamm Bowel Dis 19, 132–140 (2013). [PubMed: 22535619]
45. Dias AM et al. Dysregulation of T cell receptor N-glycosylation: a molecular mechanism involved in ulcerative colitis. Hum Mol Genet 23, 2416–2427 (2014). [PubMed: 24334766]
46. Lopez J & Grinspan A Fecal Microbiota Transplantation for Inflammatory Bowel Disease. Gastroenterology & hepatology 12, 374–379 (2016). [PubMed: 27493597]
47. Paramsothy S et al. Multidonor intensive faecal microbiota transplantation for active ulcerative colitis: a randomised placebo-controlled trial. Lancet 389, 1218–1228 (2017). [PubMed: 28214091]
48. Atarashi K et al. Th17 Cell Induction by Adhesion of Microbes to Intestinal Epithelial Cells. Cell 163, 367–380 (2015). [PubMed: 26411289]

Methods-Only References

49. Paik J et al. Potential for using a hermetically-sealed, positive-pressured isocage system for studies involving germ-free mice outside a flexible-film isolator. Gut Microbes 6, 255–265 (2015). [PubMed: 26177210]
50. Hecht G et al. A simple cage-autonomous method for the maintenance of the barrier status of germ-free mice during experimentation. Lab Anim 48, 292–297 (2014). [PubMed: 25097255]
51. Schloss PD et al. Introducing mothur: open-source, platform-independent, community-supported software for describing and comparing microbial communities. Appl Environ Microbiol 75, 7537–7541 (2009). [PubMed: 19801464]
52. Kozich JJ, Westcott SL, Baxter NT, Highlander SK & Schloss PD Development of a dual-index sequencing strategy and curation pipeline for analyzing amplicon sequence data on the MiSeq Illumina sequencing platform. Appl Environ Microbiol 79, 5112–5120 (2013). [PubMed: 23793624]
53. Segata N et al. Metagenomic biomarker discovery and explanation. Genome Biol 12, R60 (2011). [PubMed: 21702898]
54. Hirayama A et al. Metabolic profiling reveals new serum biomarkers for differentiating diabetic nephropathy. Analytical and bioanalytical chemistry 404, 3101–3109 (2012). [PubMed: 23052862]
55. Lorenz MA, Burant CF & Kennedy RT Reducing time and increasing sensitivity in sample preparation for adherent mammalian cell metabolomics. Analytical chemistry 83, 3406–3414 (2011). [PubMed: 21456517]
56. Cohen PS & Laux DC Bacterial adhesion to and penetration of intestinal mucus in vitro. Methods in enzymology 253, 309–314 (1995). [PubMed: 7476395]
57. Schulz BL, Packer NH & Karlsson NG Small-scale analysis of O-linked oligosaccharides from glycoproteins and mucins separated by gel electrophoresis. Analytical chemistry 74, 6088–6097 (2002). [PubMed: 12498206]

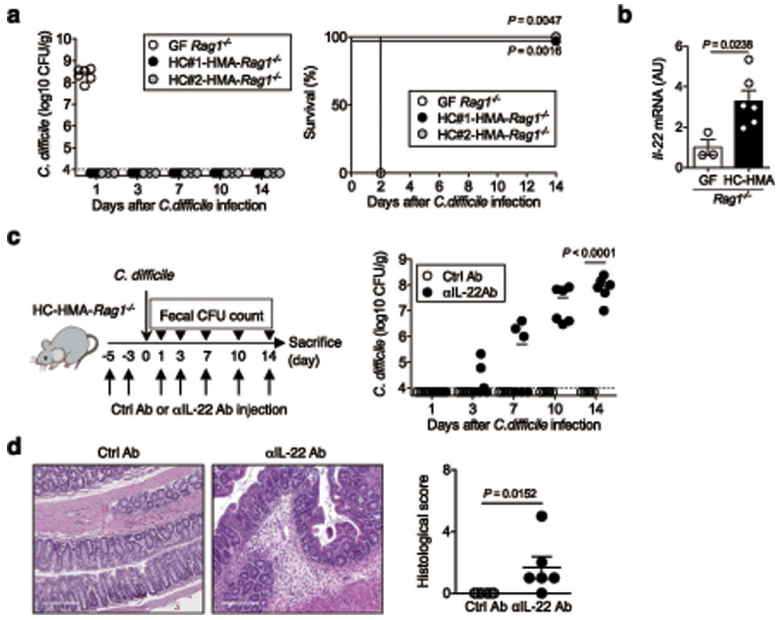

Figure 1. Healthy human microbiota-driven IL-22 prevents *C. difficile* blooms in the gut.

(**a**) (Left) GF-*Rag1*$^{-/-}$ mice were colonized with healthy microbiotas for 2 weeks (HC-HMA-*Rag1*$^{-/-}$ mice). GF or HC-HMA-*Rag1*$^{-/-}$ mice (GF: n=6, HC#1:n=5 and HC#2:n=3, biologically independent animals) were infected with *C. difficile* VPI 10463 spores (10^3 spores/mouse). *C. difficile* load in feces was determined on indicated days post-infection. Dots represent individual mice. Bars represent median. (Right) The mortality of *C. difficile* infected mice. Statistical significance was assessed by Log-rank test (two-sided). Data were pooled from two independent experiments. (**b**) *Il22* mRNA levels in GF-*Rag1*$^{-/-}$ (n=3) or HC-HMA-*Rag1*$^{-/-}$ mice (n=6) were measured by qPCR. Expression was normalized to that of the murine *Actb* gene. Data are presented as mean ± s.e.m.. Data were pooled from two independent experiments. Statistical significance was assessed by Mann-Whitney *U* test (two-sided). (**c**) *C. difficile* infected HC-HMA-*Rag1*$^{-/-}$ mice were treated with control or αIL-22 antibody twice before *C. difficile* inoculation (3 and 5 days prior to infection) and 3 times a week post-inoculation. *C. difficile* load in feces was determined on indicated days post-inoculation (n=6, biologically independent animals). Dots represent individual mice. Bars represent median. Data were pooled from two independent experiments. Statistical significance was assessed by 2-way ANOVA with Bonferroni post-hoc test (two-sided). (**d**) Representative histological images and associated histological scores. Scale bar is 200 μm. Data are presented as mean ± s.e.m.. Statistical significance was assessed by Mann-Whitney *U* test (two-sided).

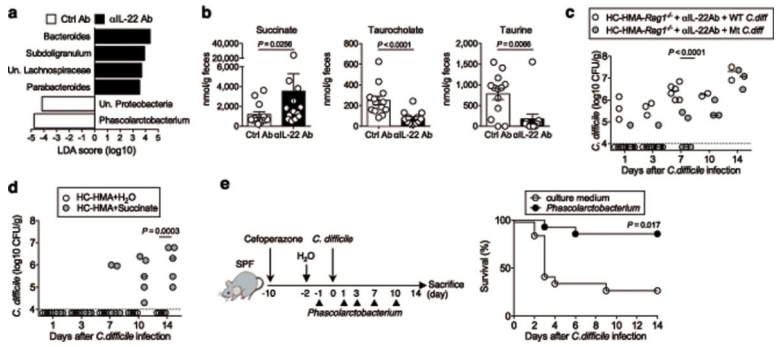

Figure 2. IL-22–mediated succinate pathway drives the colonization of *C. difficile* in the healthy microbiota.

(**a**) Fecal microbiome from HC-HMA-*Rag1*$^{-/-}$ mice treated with control or αIL-22 antibody (n=3, biologically independent animals) was analyzed. Significantly enriched bacterial taxa in αIL-22 antibody-treated mice (black bars) and control mice (white bars) were identified by LEfSe analysis. Data are representative of 2 independent experiments. (**b**) Luminal metabolites were analyzed by CE-TOF/MS. Data are presented as mean ± s.e.m. (n=13, biologically independent animals). Dots represent individual mice. Data were pooled from 3 independent experiments. Statistical significance was assessed by Mann-Whitney *U* test (two-sided). (**c**) αIL-22 antibody-treated HC-HMA-*Rag1*$^{-/-}$ mice were infected with WT JIR8094 or *Cd-CD2344*$^{-}$ mutant *C. difficile* (WT: n=7,Mut: n=8, biologically independent animals). *C. difficile* load in feces was determined on the indicated days. Dots represent individual mice. Bars represent median. Data were pooled from two independent experiments. Statistical significance was assessed by 2-way ANOVA with Bonferroni post-hoc test (two-sided). (**d**) HC-HMA-WT C57BL/6 mice were given regular water or 1% succinate. *C. difficile* load in feces was determined on the indicated days, post-inoculation. Dots represent individual mice (n=5, biologically independent animals). Bars represent median. Data were pooled from two independent experiments. Statistical significance was assessed by 2-way ANOVA with Bonferroni post-hoc test (two-sided). (**e**) Cefoperazone pre-treated SPF C57BL/6 mice were infected with *C. difficile* VPI 10463 spores (10^3 spores/mouse) by oral gavage. Mice were inoculated orally with *P. faecium* JCM 30894 and *P. succinatutens* JCM 16074 (10^6 CFU each strain) or its culture medium (n=14, biologically independent animals). The mortality of *C. difficile*–infected mice was assessed. Data were pooled from 3 independent experiments. Statistical significance was assessed by Log-rank test (two-sided).

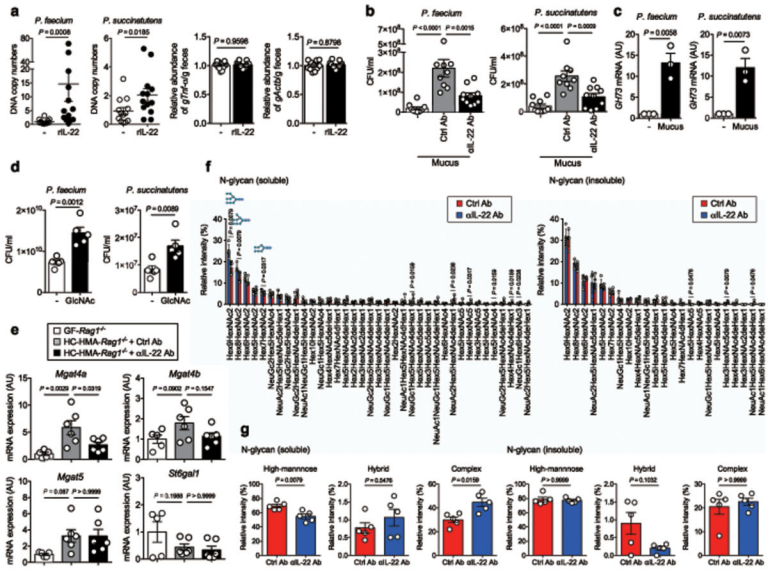

Figure 3. Host glycosylation regulated by IL-22 influences the growth of *Phascolarctobacterium* species.

(**a**) GF mice were inoculated orally with *P. faecium* JCM 30894 and *P. succinatutens* JCM 16074 (10^6 CFU each strain). Mice were then injected with either a mouse IL-22Fc fusion protein or a control Fc protein. (Left) The DNA copy numbers of *P. faecium* and *P. succinatutens* in the feces were quantified by qPCR. Each copy number was normalized to that of the host genomic DNA (murine gTnf). Relative abundance to the control group is shown. (Right) The DNA copy numbers of host genomic DNAs (murine Tnf and Actb) in the 1g of feces were quantified by qPCR. Relative abundance to the control group is shown. Dots represent individual mice. Data are presented as mean ± s.e.m. (n=13, biologically independent animals). Data were pooled from 3 independent experiments. Statistical significance was assessed by Mann-Whitney *U* test (two-sided). (**b**) *In vitro* growth of *P. faecium* and *P. succinatutens* in PYS medium supplemented with colonic mucus derived from control (n=10) or αIL-22 antibody–treated mice (n=9, independent experiments). Data are presented as mean ± s.e.m.. Dots represent independent experiments. Statistical significance was assessed by 1-way ANOVA with Bonferroni post-hoc test (two-sided). (**c**) The GH73 mRNA expression in *P. faecium* and *P. succinatutens* during the growth on mucus was analyzed by qPCR. Expression was normalized to Eubacteria 16s rRNA. Data are presented as mean ± s.e.m. (n=3 independent experiments). Statistical significance was assessed by Student *t*-test (two-sided). (**d**) *P. faecium* and *P. succinatutens* growth on GlcNAc. Data are presented as mean ± s.e.m. (n=5 independent experiments). Statistical significance was assessed by Student *t*-test (two-sided). (**e**) The expression of glycosyltransferase genes in the colonic mucosa of GF *Rag1*$^{-/-}$ (n=6, biologically independent animals) and HC-HMA-*Rag1*$^{-/-}$ mice injected with control or αIL-22 antibody was determined by qPCR. Expression was normalized to that of the murine *Actb* gene. Data are presented as mean ± s.e.m.. Data were pooled from 2 independent experiments. Statistical significance was assessed by 1-way ANOVA with Bonferroni post-hoc test (two-sided). (**f**) Colonic mucus derived from control or αIL-22 antibody–treated HMA-*Rag1*$^{-/-}$ mice were separated into GuHCl soluble and insoluble fractions. *N*-glycans were analyzed

by liquid chromatography–electrospray ionization tandem mass spectrometry. (**g**) The relative intensity of high-mannose, hybrid, and complex *N*-glycans in soluble and insoluble fractions. Data are presented as mean ± s.e.m. (n=5, biologically independent animals). Dots represent individual mice. Statistical significance was assessed by Mann-Whitney *U* test (two-sided) (**f, g**).

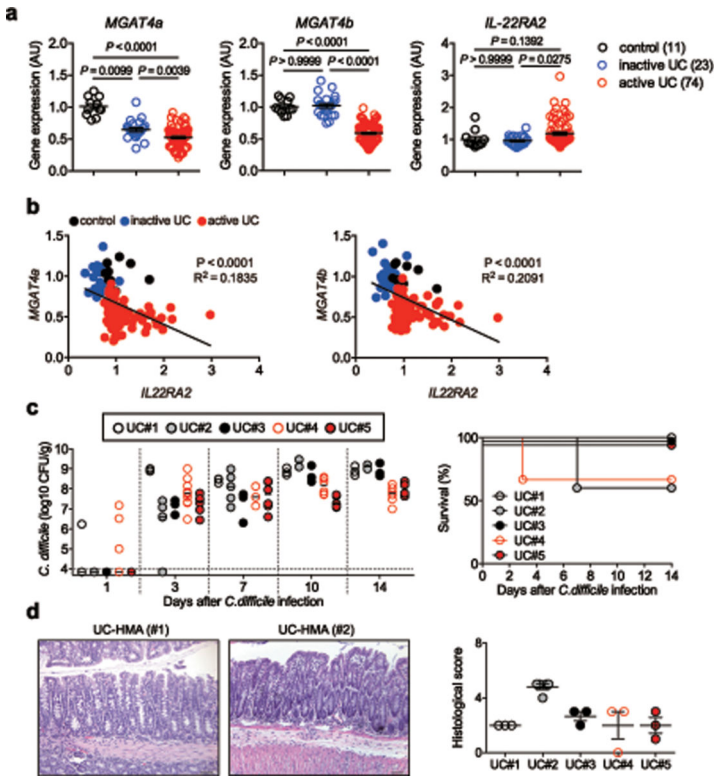

Figure 4. *N*-glycan related glycosyltransferase gene expression and CDI risk in UC patients.

(**a**) The mRNA expression of glycosyltransferase-related genes in the colonic tissue from control subjects (n=11), patients with inactive UC (n=23) and patients with active UC (n=74). Data were derived from Gene Expression Omnibus (GEO) data sets GSE75214. Dots represent biologically independent subjects. Data are presented as mean ± s.e.m.. Statistical significance was assessed by Kruskal-Wallis test with Dunn's post-hoc test (two-sided). (**b**) The correlation between *MGAT4A*/*MGAT4B* and *IL22RA2* mRNA expression in 3 groups. Statistical significance was measured by Pearson correlation test (two-sided). (**c**) GF WT C57BL/6 mice were colonized with the gut microbiotas obtained from UC patients (UC-HMA mice). UC-HMA mice were then infected with *C. difficile* VPI 10463 spores (UC#1: n=3, UC#2: n=5, UC#3: n=3, UC#4: n=9, and UC#5: n=6, biologically independent animals). *C. difficile* load in feces was determined on indicated days, post-infection. Dots represent individual mice. Bars represent median. Data were pooled from 3 independent experiments. (Right) The mortality of *C. difficile* infected UC-HMA mice. (**d**) Representative histological images and associated histological scores. Scale bar is 100 μm. Dots represent individual mice. Data are presented as mean ± s.e.m. (n=3, biologically independent animals) from pooled 3 independent experiments.

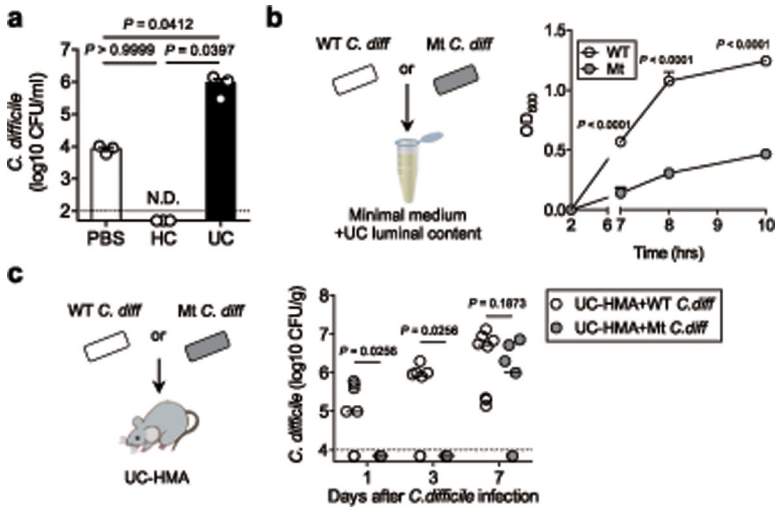

Figure 5. *C. difficile* utilizes luminal succinate for its growth in UC patients.

(a) *Ex vivo* germination and growth of *C. difficile* strain VPI 10463 in cecum contents isolated from HC-HMA and UC-HMA mice (n=3 biological independent animals). Data are presented as mean ± s.e.m. from pooled 3 independent experiments. Statistical significance was assessed by 1-way ANOVA with Bonferroni post-hoc test (two-sided). (**b**) *Ex vivo* germination and growth of WT or *Cd-CD2344*$^{-}$ mutant *C. difficile* in UC luminal contents. Data are presented as mean ± s.d. (n=3 technical replicates). Data are representative of 3 independent experiments. Statistical significance was assessed by 2-way ANOVA with Bonferroni post-hoc test (two-sided). (**c**) UC-HMA mice were infected with WT or *Cd-CD2344*$^{-}$ mutant *C. difficile* (WT: n=8, Mut: n=7, biologically independent animals). *C. difficile* load in feces was determined on indicated days post-infection. Dots represent individual mice. Bars indicate median. Data were pooled from 3 independent experiments Statistical significance was assessed by 2-way ANOVA with Bonferroni post-hoc test (two-sided).

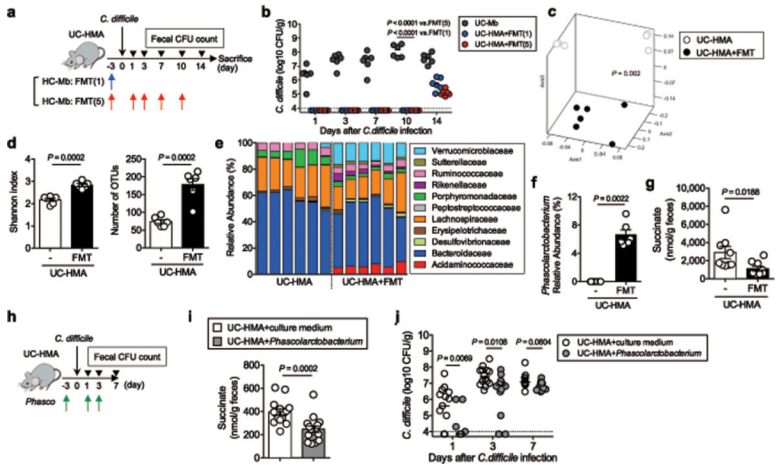

Figure 6. Restoration of luminal metabolites reduces the risk of *C. difficile* infection.

(**a-g**) UC-HMA mice were infected with *C. difficile* VPI 10463 spores (10^3 spores/mouse). Mice were transplanted with a healthy, human-derived fecal microbiota (FMT) (n=6, biologically independent animals). (**b**) *C. difficile* load in feces. Dots represent individual mice. Bars indicate median. Data were pooled from 2 independent experiments. Statistical significance was assessed by 2-way ANOVA with Bonferroni post-hoc test (two-sided). (**c-f**) Fecal microbiota before CDI (day 0) was harvested and bacterial 16S rRNA sequences were analyzed. (**c**) Microbial community structures were analyzed using the Yue and Clayton dissimilarity distance metric (θ_{YC}). Statistical significance was assessed by AMOVA test (two-sided) (**d**) Shannon index (α-diversity) and number of OTUs (richness). Data are presented as mean ± s.d. (n=6, biologically independent animals). Statistical significance was assessed by Mann-Whitney *U* test (two-sided). (**e**) Bacterial taxonomy at the family level in the feces. (**f**) The relative abundance of *Phascolarctobacterium* species in the feces. Data are presented as mean ± s.d. (n=6 each). Statistical significance was assessed by Mann-Whitney *U* test (two-sided). (**g**) Fecal succinate concentration at day 0 was analyzed by CE-TOF/MS. Data are presented as mean ± s.d. (n=9, biologically independent animals). Dots represent individual mice. Data were pooled from 2 independent experiments. Statistical significance was assessed by Mann-Whitney *U* test (two-sided). (**h-j**) UC-HMA mice were infected with *C. difficile* VPI 10463 spores (10^3 spores/mouse). Mice were inoculated with *P. faecium* JCM 30894 and *P. succinatutens* JCM 16074 (10^6 CFU each strain). (**i**) Luminal succinate concentration was analyzed by LC-MS. Data are presented as mean ± s.d. (n=15, biologically independent animals) from pooled 3 independent experiments. Statistical significance was assessed by Mann-Whitney *U* test (two-sided). (**j**) *C. difficile* load in feces. Data are presented as mean ± s.d. (n=15, biologically independent animals) from pooled 3 independent experiments. Statistical significance was assessed by 2-way ANOVA with Bonferroni post-hoc test (two-sided).